




# Genetic architecture reconciles linkage and association studies of complex traits

Received: 26 February 2023

Accepted: 30 August 2024

Published online: 7 October 2024

 Check for updates

Julia Sidorenko <sup>1</sup>✉, Baptiste Couvy-Duchesne<sup>1,2,3</sup>, Kathryn E. Kemper <sup>1</sup>, Gunn-Helen Moen<sup>1,4,5,6</sup>, Laxmi Bhatta<sup>5</sup>, Bjørn Olav Åsvold <sup>5,7,8</sup>, Reedik Mägi<sup>9</sup>, Estonian Biobank Research Team\*, Alireza Ani <sup>10,11</sup>, Rujia Wang <sup>10</sup>, Ilja M. Nolte <sup>9</sup>, Lifelines Cohort Study\*, Scott Gordon <sup>2</sup>, Caroline Hayward <sup>12</sup>, Archie Campbell <sup>13</sup>, Daniel J. Benjamin <sup>14,15,16</sup>, David Cesarini <sup>16,17,18</sup>, David M. Evans <sup>1,6,19</sup>, Michael E. Goddard<sup>20,21</sup>, Chris S. Haley<sup>22,23,24</sup>, David Porteous <sup>12</sup>, Sarah E. Medland <sup>2</sup>, Nicholas G. Martin <sup>2</sup>, Harold Snieder <sup>10</sup>, Andres Metspalu <sup>9</sup>, Kristian Hveem<sup>5,7</sup>, Ben Brumpton <sup>5,7</sup>, Peter M. Visscher <sup>1,25,26</sup> ✉ & Loic Yengo<sup>1,26</sup> ✉

Linkage studies have successfully mapped loci underlying monogenic disorders, but mostly failed when applied to common diseases. Conversely, genome-wide association studies (GWASs) have identified replicable associations between thousands of SNPs and complex traits, yet capture less than half of the total heritability. In the present study we reconcile these two approaches by showing that linkage signals of height and body mass index (BMI) from 119,000 sibling pairs colocalize with GWAS-identified loci. Concordant with polygenicity, we observed the following: a genome-wide inflation of linkage test statistics; that GWAS results predict linkage signals; and that adjusting phenotypes for polygenic scores reduces linkage signals. Finally, we developed a method using recombination rate-stratified, identity-by-descent sharing between siblings to unbiasedly estimate heritability of height ( $0.76 \pm 0.05$ ) and BMI ( $0.55 \pm 0.07$ ). Our results imply that substantial heritability remains unaccounted for by GWAS-identified loci and this residual genetic variation is polygenic and enriched near these loci.

Genetic studies of human complex traits have progressed from using pedigree designs (for example, twin studies<sup>1</sup>) to estimating heritability from population-based genomic surveys for dissecting genetic variation at the level of individual loci. In between, there was a period of two decades (roughly from 1985 to 2005) where researchers used pedigree-based, genome-wide linkage scans to map disease loci. Linkage analysis is an experimental design that studies the segregation of markers and phenotypes within a pedigree to map trait loci. It is robust to confounding effects caused by population stratification and requires only sparse marker maps, but is also low in power and mapping resolution, the latter because there are very few recombination

events within a pedigree<sup>2,3</sup>. Linkage analyses have been highly successful in mapping single-gene Mendelian disorders<sup>4</sup>. Linkage studies of complex traits were predicated on the success of mapping single-gene disorders and major risk loci affecting common diseases such as breast cancer<sup>5</sup> and Alzheimer's disease<sup>6</sup>. However, linkage studies for most common diseases and other complex traits were largely a disappointment in that they failed to produce robust and replicable results<sup>7</sup>. Many explanations have been given in the literature for this failure, including 'genetic heterogeneity' (family-specific genetic loci causing disease) and statistical artefacts resulting from model selection, insufficient correction for multiple testing and small sample sizes. The

A full list of affiliations appears at the end of the paper. \*Lists of authors and their affiliations appear at the end of the paper.

✉ e-mail: [j.sidorenko@imb.uq.edu.au](mailto:j.sidorenko@imb.uq.edu.au); [peter.visscher@uq.edu.au](mailto:peter.visscher@uq.edu.au); [lyengo@imb.uq.edu.au](mailto:lyengo@imb.uq.edu.au)

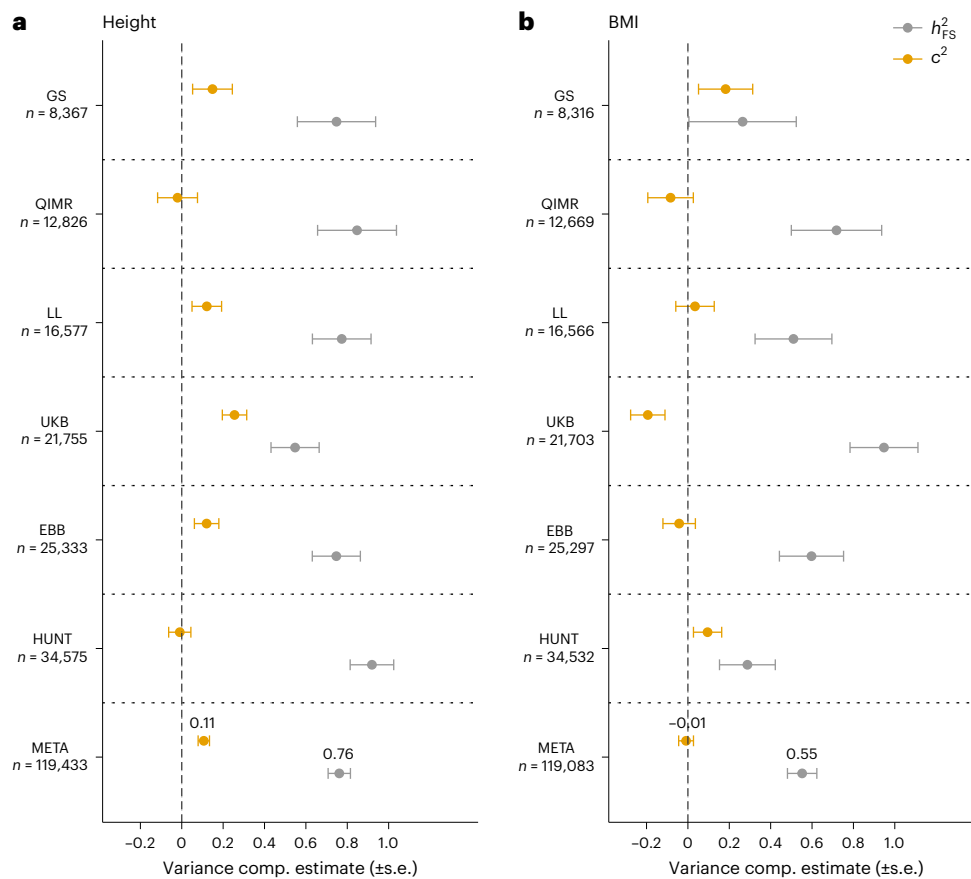


**Fig. 1** | RR-stratified estimates of heritability ( $h_{FS}^2$ ) and proportion of variance owing to common sibling effects are not correlated with IBD sharing for height and BMI. **a, b**, RR-stratified estimates of heritability and proportion of variance caused by common sibling effects uncorrelated with IBD sharing ( $c^2$ ) for height (**a**) and BMI (**b**). Estimates were obtained using restricted maximum likelihood in six cohorts of European ancestry individuals: the UKB,

GS, LL, QIMR, EBB, HUNT and the fixed-effect meta-analysis results combining all cohorts (META). The number of quasi-independent sib-pairs ( $n$ ) for each trait and cohort is indicated on the y axis. Each dot represents a point estimate and the corresponding error bar represents its s.e. Numeric values are given in Supplementary Table 6a. Estimated variance components (comp.) were not constrained to be positive to ensure unbiasedness.

lack of power and mapping resolution of linkage studies prompted the development of GWASs<sup>2</sup>.

Despite initial skepticism that GWASs would lead to marker-trait discoveries (for example, refs. 8,9), GWASs based on common SNP markers have been highly successful in detecting robust associations between SNPs and complex traits. Yet, SNPs tested for association in standard GWASs capture only a third to a half of the genetic variation estimated from pedigree data<sup>9</sup>. The polygenicity and effect size distribution of the genetic variation not accounted for by GWASs remain uncertain. Even after early GWAS results, it was hypothesized that family-specific rare mutations of large effect could explain a substantial fraction of common and complex human diseases such as schizophrenia<sup>10</sup>. Although this view has remained controversial<sup>11,12</sup>, it remains possible that certain genomic loci harbor multiple penetrant alleles with effects that cannot be fully captured in a GWAS but are detectable using a linkage design. Such loci might also contain common variants already detected by GWASs. The architecture of the genetic variation unaccounted for by GWASs determines what experimental design is best for its discovery and dissection. For example, if common variation acts on phenotypes through gene expression networks that ultimately affect gene regulation at a small number of core genes<sup>13</sup>, then residual genetic variation caused by rare variants may concentrate on those core genes in *cis*, and either large-scale, population-based, exome sequencing studies or large-scale, family-based linkage studies may identify such genes. In contrast, if residual genetic variation is just as polygenic as common genetic variance, then large-scale,

population-based, whole-genome sequencing studies would be best for variant discovery.

Family-based designs combined with dense genome-wide marker (SNP) data can be used to address a number of questions that neither pedigree nor GWAS designs alone can answer. They can be used to estimate genetic variance within families by exploiting the variation in actual relatedness around its expectation, resulting in estimates of heritability free from confounding owing to population stratification and other sources of biases<sup>14,15</sup>. Estimates of SNP effects within families are likewise unaffected by population stratification and can be contrasted with between-family estimates from population-based studies to dissect direct from indirect genetic effects<sup>16,17</sup> and to estimate the effect of nonrandom mating<sup>18</sup>.

In the present study, we used data from  $n = 119,457$  sibling pairs (sib-pairs) from six large cohorts of European ancestry participants (Generation Scotland<sup>19</sup> (GS,  $n = 8,368$ ), the Queensland Institute of Medical Research cohort (QIMR,  $n = 12,844$ ), the Lifelines Cohort Study<sup>20,21</sup> (LL,  $n = 16,836$ ), the UK Biobank<sup>22</sup> (UKB,  $n = 21,756$ ), the Estonian Biobank<sup>23</sup> (EBB,  $n = 25,333$ ) and the Trøndelag Health Study<sup>24,25</sup> (HUNT,  $n = 34,575$ )). We estimated genome-wide and locus-specific genetic variation for height and BMI and assessed, through theory, simulation and analysis of real data, the consistency between linkage and population-based association studies. We investigated how genome-wide identity-by-descent (IBD) estimators from SNP data can yield biased heritability estimates under recombination rate (RR)-dependent genetic architectures and propose that RR-stratified analysis is a robust approach to reduce or eliminate this bias. We estimated a total heritability that is consistent

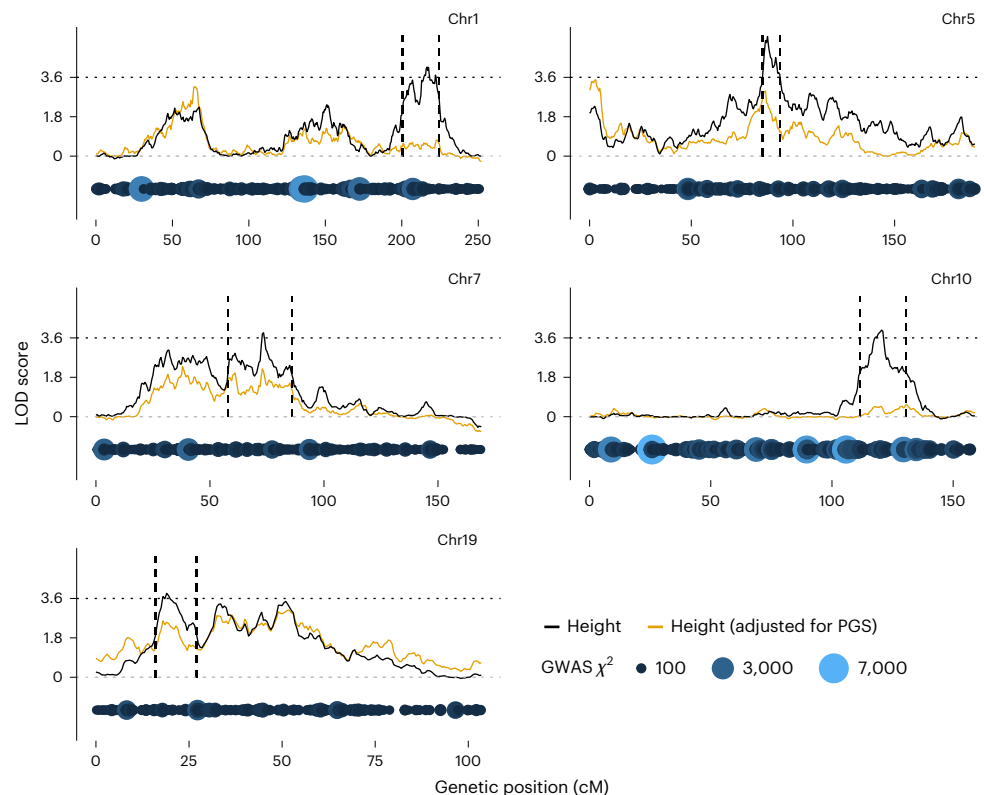


**Fig. 2 | Chromosomes containing loci significantly linked with height.**

Linked loci were identified from the meta-analysis of 119,457 QISPs before and after adjustment for genetic predictors (PGS) derived from the largest available GWAS of height<sup>33</sup> (average proportion of height variance explained across cohorts:  $R^2 = 0.38$ ). The genetic position of independent trait-associated SNPs is represented below the  $y = 0$  line by blue dots, the radius of which is proportional

to the association  $\chi^2$  statistic. Results for all the autosomes for height and BMI are shown in Supplementary Fig. 4a,b. The vertical dashed lines indicate the two LOD drop-off CIs (relative to the peak LOD score) on each side of a genetic position where the linkage LOD score exceeds 3.6 (Table 1). The black horizontal dotted line represents the threshold for significantly linked loci (LOD score  $\geq 3.6$ ). The gray horizontal dashed line indicates an LOD score of 0.

with that of pedigree (twin) studies and about twofold larger than that captured from common SNPs in GWASs, implying that a substantial proportion of genetic variation in the human genome is not captured by the common variant GWAS paradigm. We provided evidence that the residual genetic variation is also polygenic.

## Results

### Estimates of heritability from IBD regression

**RR-dependent biases in IBD regression.** We used the IBD regression method<sup>14,26</sup> to partition the phenotypic correlation between siblings ( $r = 0.48$  for height and  $r = 0.27$  for BMI; Supplementary Table 1) into a genetic and a shared environment component. Classically, this method quantifies genome-wide IBD sharing as a fraction of the length of the genome measured in centimorgan (cM) units, which implicitly upweights the contribution of loci with high RRs. Alternatively, genome-wide IBD sharing could be quantified as the proportion of DNA base-pairs shared between relatives. The latter approach implicitly assumes independence between RR and the genomic distribution of genetic variance.

We tested these two implicit assumptions through simulations and found that using either measure of IBD sharing can lead to biased heritability estimates when the genomic distribution of causal variants depends on RR (Supplementary Note, Supplementary Figs. 1 and 2 and Supplementary Tables 2–5), as shown previously using population-based designs<sup>27</sup>. To remedy this problem, we proposed an RR-stratified estimation method to account for variation in IBD sharing between loci with different RRs. Briefly, our method (1) groups genomic loci across the genome into four classes of homogeneous RR loci, (2) quantifies the average IBD sharing at each class, (3) estimates the contribution of each

class to the phenotypic correlation between siblings and then (4) sums up those contributions to obtain a final estimate of heritability (more details in Supplementary Note). We show through simulations that RR-stratified estimation is robust to differences in RRs between markers and unobserved causal variants (Supplementary Table 5). Therefore, we hereafter report only results obtained with this approach. For comparison, we also report unstratified results in Supplementary Table 6.

**RR-stratified estimates of heritability.** The parameters of our RR-stratified IBD regression model include the sum of RR-stratified, full-sib IBD heritability (hereafter denoted  $h_{FS}^2$ ) and the proportion of variance due to effects common to siblings and independent of IBD sharing (hereafter denoted  $c^2$ ). Estimates of  $h_{FS}^2$  and  $c^2$  (hereafter denoted  $\hat{h}_{FS}^2$  and  $\hat{c}^2$ , respectively) were obtained using unconstrained (that is, estimates are allowed to be negative to ensure unbiasedness), restricted, maximum likelihood (Methods) in each cohort. We then performed an inverse-variance-weighted meta-analysis to combine estimates across cohorts (Fig. 1 and Supplementary Table 6a). Heritability estimates across cohorts were largely consistent for height (Cochran's heterogeneity  $Q$  statistic  $P = 14.5\%$ ,  $P_{HET} = 0.32$ ), but showed moderate heterogeneity for BMI ( $P = 56.8\%$ ,  $P_{HET} = 0.04$ ). The meta-analyzed estimates of  $\hat{h}_{FS}^2$  were high for both height ( $\hat{h}_{FS}^2 = 0.76$ , s.e. = 0.05) and BMI ( $\hat{h}_{FS}^2 = 0.55$ , s.e. = 0.07), consistent with large heritability estimates from twin studies<sup>1,28,29</sup>. We found a significant nonzero  $\hat{c}^2$  for height ( $\hat{c}^2 = 0.11$ , s.e. = 0.03) but not for BMI ( $\hat{c}^2 = -0.01$ , s.e. = 0.04), although both estimates showed moderate heterogeneity across cohorts (height:  $P = 61.7\%$ ,  $P_{HET} = 0.02$ ; BMI:  $P = 51.3\%$ ,  $P_{HET} = 0.07$ ). A significantly positive  $\hat{c}^2$  could be the result of either assortative mating or shared environmental effects, or both. We show in

**Table 1 | Genomic regions significantly linked with height**

Chr	Start (bp)	Stop (bp)	Length (Mb)	Start (cM)	Stop (cM)	Length (cM)	Max. LOD score	Proportion of genes in peak	Proportion of trait-associated SNPs in peak
1	213,682,673	234,840,374	21.2	200.5	224.5	24	4.1	163 of 2,566	119 of 970
5	78,955,590	89,401,919	10.4	85.0	93.5	8.5	5.5	50 of 1,172	37 of 742
7	42,401,253	81,189,104	38.8	58.0	86.0	28	3.8	271 of 1,235	131 of 673
10	104,479,048	122,171,602	17.7	111.5	130.5	19	4.0	118 of 990	69 of 558
19	4,196,471	8,360,632	4.2	16.0	27.0	11	3.8	120 of 1,806	43 of 375

Linkage peaks were defined using the two LOD drop-off method on each side of a genetic position, where the linkage LOD score > 3.6. Proportion of genes (or trait-associated SNPs) in peaks is defined relative to the number of genes (or trait-associated SNPs) on the chromosome (Chr). Genomic positions correspond to the hg19 genome build.

Supplementary Note that the significant  $\hat{c}^2$  observed for height can be mostly explained by assortative mating, thus leaving little room for other effects. We repeated all analyses using rank-based transformed traits and found highly consistent results (Supplementary Table 6b).

### Locus-specific linkage analysis of height and BMI

Next, we performed a locus-by-locus linkage analysis to quantify the amount of variation explained by IBD status at 0.5-cM spaced loci across each autosome. As before, we analyzed each cohort separately and then meta-analyzed locus-specific linkage signals across cohorts. The mean linkage test statistic ( $\chi^2$ ) across genomic locations was 3.43 (s.e. = 0.38) for height and 1.43 (s.e. = 0.22) for BMI, consistent with estimates of  $h_{FS}^2$  (Methods, Extended Data Fig. 1 and Supplementary Table 7a) and the effective number of independent genomic segments (Supplementary Table 8). Analyses of rank-based transformed traits yielded similar results (Supplementary Table 7b and Supplementary Fig. 3). We detected five loci on chromosomes 1, 5, 7, 10 and 19 showing significant linkage with height (Fig. 2 and Table 1; for all chromosomes, see Supplementary Fig. 4a), but none for BMI (Supplementary Fig. 4b). The statistical significance of linkage signals was determined using 3.6 as the threshold for the logarithm of the odds (LOD) score, as previously suggested for genome-wide significance in linkage studies<sup>30</sup>. This threshold corresponds to a  $P$  value of  $2.2 \times 10^{-5}$ .

For each locus, we defined a confidence interval (CI) for the location of the underlying causal variants using the ‘two LOD drop-off’ method<sup>31</sup> (Methods). We conservatively chose a two-unit LOD score drop-off to ensure a coverage of at least 95%. The length of these five CIs varied between 4.2 Mb (height-linked locus: chr19: 4,196,471–8,360,632; genomic position in build hg19) and 38.8 Mb (height-linked locus: chr7: 42,401,253–81,189,104), which remained quite broad despite a sample size of >119,000 sib-pairs (Table 1).

In summary, we confirmed that widespread genetic variation underlies height and BMI and detected five loci showing significant linkage with height.

### GWAS and linkage results are significantly correlated

**Overview of the predLINK method.** We developed a method, predLINK, to predict the variance explained at a given locus from a linkage genome scan. The predicted linkage signal is calculated as a sum of variances explained at all neighboring causal (or trait-associated) loci weighted by their genetic distance to the locus of interest (equation (1); Methods). This method builds on previous work in which the theoretical expectation of the genetic variance captured by a marker was derived for a linkage analysis in an outbred population under an infinitesimal architecture<sup>32</sup>. We assessed the performance of predLINK using the correlation ( $\hat{\phi}$ ) between the observed and predicted variance explained at 0.5-cM spaced loci across each chromosome.

**PredLINK applied to simulated data.** We first performed large-scale simulations of up to 100,000 sib-pairs to validate predLINK under various polygenic architectures. Overall, we found the largest correlation

between the theoretically predicted (Extended Data Fig. 2a,b, black line) and observed linkage signals (Extended Data Fig. 2a,b, yellow and gray lines) for traits where the genetic variance is contributed by just a few causal variants with large effects and that it decreased with higher trait polygenicity (Extended Data Fig. 2a–c, left to right) and with a smaller discovery sample size (Extended Data Fig. 2a–c, yellow versus gray lines). The mean  $\hat{\phi}$  across 100 replicates for the least polygenic genetic architecture was 0.91 (s.e. = 0.02) and 0.69 (s.e. = 0.04) in the linkage analyses of 100,000 and 20,000 sib-pairs, respectively (Extended Data Fig. 2c, left-most panel, enlarged symbols, and Supplementary Table 9) and decreased to 0.34 (s.e. = 0.00) and –0.01 (s.e. = 0.00), for the infinitesimal model (Extended Data Fig. 2c, right-most panel, enlarged symbols, and Supplementary Table 9). Moreover, we found that errors in estimated SNP effects slightly decrease  $\hat{\phi}$ , especially when polygenicity is low (Extended Data Fig. 2c and Supplementary Table 9).

**PredLINK applied to height and BMI.** Next, we applied predLINK to assess the colocalization of observed and predicted linkage signals from GWASs, using 12,111 and 795 genome-wide significant SNPs associated with height<sup>33</sup> and BMI (Supplementary Data), respectively (Methods). The 795 genome-wide significant SNPs associated with BMI were obtained from re-analyzing data from ref. 34 after excluding sib-pairs (and their close relatives) from the UKB also included in our linkage analyses (Methods). For height, the per-chromosome  $\hat{\phi}$  ranged from 0.11 to 0.93, with a length-weighted (length measured in cM) average across chromosomes of  $\hat{\phi} = 0.51$  (s.e. = 0.05) (Supplementary Fig. 5a and Supplementary Table 10). We found a smaller correlation  $\hat{\phi} = 0.29$  (s.e. = 0.08) for BMI (Supplementary Fig. 5b and Supplementary Table 10), consistent with a lower power to detect association and linkage for BMI compared with height (Supplementary Note, Supplementary Figs. 6–8 and Supplementary Tables 9 and 11).

**Curvature effect.** Under an infinitesimal genetic architecture, stronger linkage signals are expected at the center of a chromosome compared with its ends<sup>35</sup>. This is the result of centrally located markers being in linkage with more causal variants than those located terminally, which appears as a curved linkage signal (Extended Data Fig. 2a,b). Given that predLINK recapitulates such intrinsic curvature of linkage signals, a nonzero  $\hat{\phi}$  is expected for polygenic traits such as height and BMI. We call this the ‘curvature effect’ (CE). As an empirical illustration of this CE, we observed a significant colocalization not only between height-associated SNPs and linkage signals for height ( $\hat{\phi} = 0.51$ , s.e. = 0.05; Fig. 3a), but also between height-associated SNPs and linkage signals for BMI ( $\hat{\phi} = 0.19$ , s.e. = 0.10; Fig. 3b and Supplementary Table 10). Similarly, we found a significant colocalization between BMI-associated SNPs and linkage signals for height ( $\hat{\phi} = 0.37$ , s.e. = 0.08; Fig. 3c and Supplementary Table 10). This observation cannot be explained by pleiotropy alone, given the low genetic correlation between height and BMI<sup>36</sup> ( $r_G = -0.10$ ).

To assess the significance of  $\hat{\phi}$  beyond the expected correlation owing to the CE ( $\hat{\phi}_{CE}$ ), we generated a null distribution from predicted

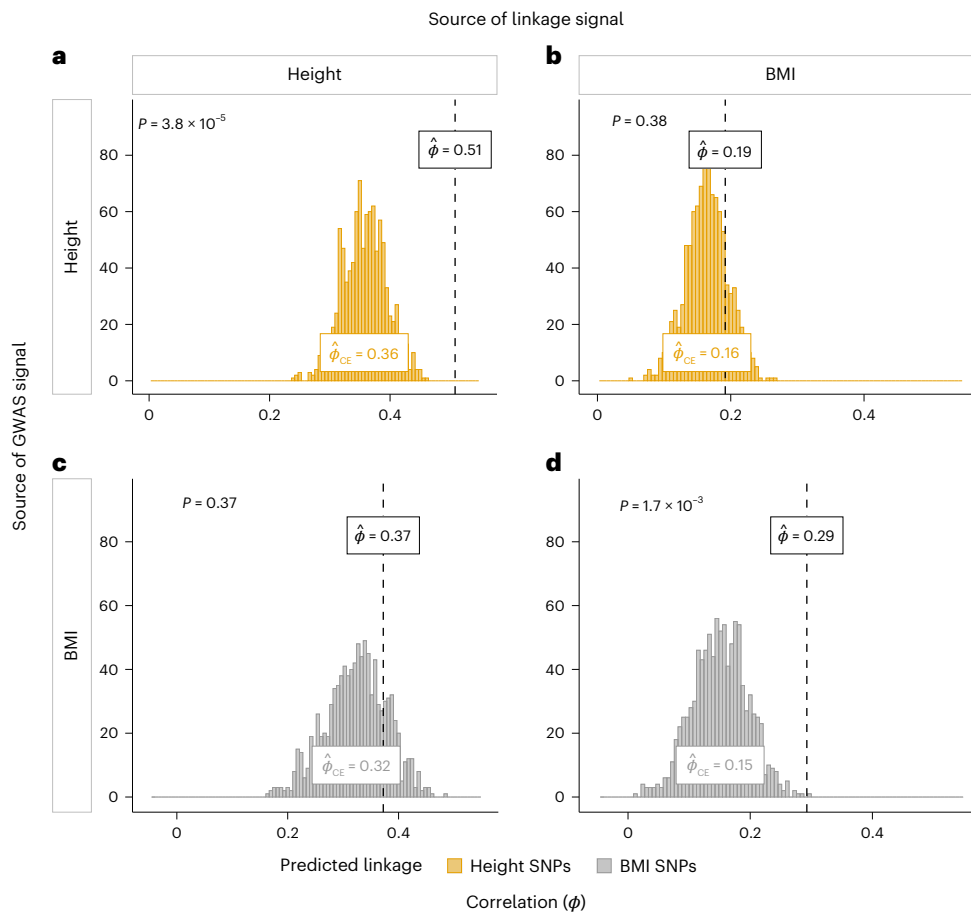


**Fig. 3 | Colocalization between observed and GWAS-predicted linkage signals. a–d,** Row panels (row 1 (a and b), row 2 (c and d)) representing predicted linkage signals based on a given set of trait-associated SNPs and column panels representing observed linkage signals for height (a and c) and BMI (b and d). The x axis in each panel displays the correlation ( $\hat{\phi}$ ) between observed and predicted (from GWAS results; Methods) linkage signals. The y axis represents counts. In each panel, the vertical dashed line represents the correlation between observed linkage signals for the trait specified in the corresponding column panel header and predicted linkage signals from either 12,010 height-associated SNPs (a and b) or 787 BMI-associated SNPs (c and d). Predicted linkage signals were also obtained under the null hypothesis (that is, ‘the correlation between observed and predicted linkage signals is due to the curvature effect’) using 1,000 draws of random SNPs with similar MAF and LD properties to trait-associated SNPs. The

histogram in each panel represents the distribution of correlations (under the null) between observed linkage for the trait indicated in the corresponding column panel and predicted linkage obtained from these 1,000 draws. The mean of correlations obtained under the null hypothesis is denoted  $\hat{\phi}_{CE}$ . The  $P$  values reported in the top-left corner of each panel assess the statistical significance of the difference between  $\hat{\phi}$  and  $\hat{\phi}_{CE}$  using a two-sided Wald’s test (conditional on  $\hat{\phi}$ ) and based on the sampling variance of  $\hat{\phi}_{CE}$  across replicates. At a significance threshold  $P < 0.05$ , our results imply that linkage signals for height are predictable from height-associated SNPs (a), but not from BMI-associated SNPs (c) and that linkage signals for BMI are also predictable from BMI-associated SNPs (d), but not from height-associated SNPs (b). Numeric values are presented in Supplementary Table 10.

linkage based on random SNPs matched on minor allele frequency (MAF) and linkage disequilibrium (LD) with the actual trait-associated SNPs. For height, the average  $\hat{\phi}_{CE}$  over 1,000 sets of 12,010 random SNPs was  $\hat{\phi}_{CE} = 0.36$  (s.e. = 0.04), which is significantly lower than  $\hat{\phi} = 0.51$  (s.e. = 0.05) obtained using height-associated SNPs (Wald’s test  $P$  value:  $P_{Wald} = 3.8 \times 10^{-5}$ ; Fig. 3a and Supplementary Table 10) and implies that predLINK can significantly predict a height-specific linkage signal over and above the CE. The same was true for BMI, where the observed  $\hat{\phi} = 0.29$  (s.e. = 0.08) was significantly higher than  $\hat{\phi}_{CE} = 0.15$  (s.e. = 0.05) obtained over 1,000 sets of 787 random SNPs ( $P_{Wald} = 1.7 \times 10^{-3}$ ; Fig. 3d and Supplementary Table 10). Overall, these results show that the colocalization between GWAS and linkage signals for height and BMI is only partially explained by the high polygenicity of these two traits.

#### A polygenic missing heritability enriched near GWAS loci

We hypothesized that, if concordance between linkage and association results is the result of the same genetic loci, then correcting phenotypes for polygenic scores (PGSs) should reduce the test statistic for linkage. We focused on height to test this hypothesis and used a PGS based on

12,111 height-associated variants<sup>33</sup> explaining 0.35–0.41 (weighted mean = 0.38; Table 2) of phenotypic variance in our cohorts. After adjustment for the PGS, estimates of  $h_{FS}^2$  and  $c^2$  were  $\hat{h}_{FS}^2 = 0.68$  (s.e. = 0.06) and  $\hat{c}^2 = 0.08$  (s.e. = 0.03), and the average test statistic decreased from 3.43 (s.e. = 0.38) to 2.2 (s.e. = 0.28) (Table 2), implying that ~51% (that is,  $(1 - (2.2 - 1))/(3.43 - 1)$ ) of the height genetic variance in linkage analysis is captured by height-associated SNPs. Importantly, the proportion of height variance explained by each chromosome remained significantly correlated with chromosome length before and after adjustment for the PGS (before adjustment: 0.73 (s.e. = 0.17); after PGS adjustment: 0.61 (s.e. = 0.22); Fig. 4), implying that the unaccounted genetic variance for height is also polygenic. Finally, adjustment for the PGS reduced LOD scores to  $< 3.6$  at all height-linked loci (Fig. 2).

Next, we estimated the correlation between linkage signals for PGS-adjusted height and predicted linkage signals from height-associated SNPs. We found a correlation  $\hat{\phi} = 0.38$  (s.e. = 0.08), significant beyond the expected CE ( $\hat{\phi}_{CE} = 0.26$ , s.e. = 0.03,  $P_{Wald} = 2.2 \times 10^{-4}$  testing the difference between  $\hat{\phi}$  and  $\hat{\phi}_{CE}$ ; Extended

**Table 2 | Estimates from linkage analyses of PGS-adjusted traits**

Trait		GS	QIMR	LL	UKB	EBB	HUNT	Meta-analysis
Height	$h_{\text{SNP}}^2$	0.44 (0.03)	0.43 (0.04)	0.48 (0.01)	0.50 (0.01)	0.52 (0.02)	0.50 (0.01)	0.50 (0.01)
	$R_{\text{PGS}}^2$	0.41 (0.009)	0.35 (0.009)	0.38 (0.006)	0.41 (0.005)	0.37 (0.005)	0.39 (0.005)	0.38 (0.002)
	Mean $\chi^2$ (s.e.)	1.05 (0.17)	1.02 (0.13)	1.20 (0.18)	1.01 (0.13)	1.34 (0.16)	1.09 (0.15)	2.2 (0.28)
	Median $\chi^2$	0.87	1.22	1.13	1.14	1.64	1.18	2.44
	Proportion $\chi^2 > 0$	0.62	0.65	0.67	0.62	0.74	0.74	0.84
	$\widehat{h}_{\text{FS}}^2$ (s.e.)	0.76 (0.21)	0.80 (0.21)	0.71 (0.15)	0.45 (0.13)	0.81 (0.13)	0.67 (0.12)	0.68 (0.06)
Height (PGS adjusted)	$\widehat{c}^2$ (s.e.)	0.08 (0.11)	-0.10 (0.11)	0.11 (0.08)	0.25 (0.07)	0.02 (0.07)	0.05 (0.06)	0.08 (0.03)
	$h_{\text{SNP}}^2$	0.26 (0.03)	0.25 (0.04)	0.27 (0.01)	0.26 (0.01)	0.30 (0.02)	0.25 (0.01)	0.26 (0.01)
	$R_{\text{PGS}}^2$	0.11 (0.006)	0.09 (0.006)	0.10 (0.004)	0.10 (0.003)	0.09 (0.003)	0.08 (0.003)	0.09 (0.002)
	Mean $\chi^2$ (s.e.)	0.84 (0.11)	0.87 (0.14)	0.68 (0.09)	1.01 (0.15)	0.77 (0.11)	1.04 (0.16)	1.39 (0.21)
	Median $\chi^2$	0.95	0.85	0.72	0.99	0.64	0.99	1.38
	Proportion $\chi^2 > 0$	0.54	0.61	0.58	0.71	0.62	0.62	0.76
BMI (PGS adjusted)	$\widehat{h}_{\text{FS}}^2$ (s.e.)	0.26 (0.27)	0.75 (0.22)	0.44 (0.19)	0.96 (0.17)	0.70 (0.16)	0.33 (0.14)	0.58 (0.07)
	$\widehat{c}^2$ (s.e.)	0.15 (0.13)	-0.14 (0.11)	0.04 (0.1)	-0.23 (0.09)	-0.12 (0.08)	0.05 (0.07)	-0.05 (0.04)

$R_{\text{PGS}}^2$  denotes the prediction accuracy of the PGS in each cohort measured by the squared correlation between the trait and the PGS. Approximated s.e. values for  $R_{\text{PGS}}^2$  were obtained using the delta method. The mean test statistic for linkage is denoted as  $\chi^2$ . The s.e. values denoted as s.e.  $\widehat{h}_{\text{FS}}^2$  and  $\widehat{c}^2$  were obtained using recombination rate stratified estimation. Note that three significant digits were used to report s.e. values for  $R_{\text{PGS}}^2$  because of the larger precision of  $R_{\text{PGS}}^2$  estimates relative to that of heritability estimates.

Data Fig. 3 and Supplementary Table 10), which provides evidence that causal variants for height not captured by current GWASs are also enriched within GWAS-detected, height-associated loci.

In conclusion, our results support the hypothesis that the same genetic loci underlie association and linkage signals, and suggest that the missing heritability of height is polygenic and involves causal variants enriched near height-associated SNPs identified through large-scale GWASs.

## Discussion

We conducted a large linkage analysis of complex traits in humans using -119,000 sib-pairs. We first estimated the variance explained by degree of IBD sharing across the entire genome and subsequently estimated the variance explained by IBD sharing at specific loci across the genome (a traditional linkage scan across the genome). We estimated a heritability of 0.76 (s.e. = 0.05) and 0.55 (s.e. = 0.07) for height and BMI, respectively, and detected multiple significant linkage peaks for height. Analyses were repeated after adjusting the phenotype for known population-wide associations from GWASs, using a PGS, and this showed a reduction both of the heritability and in the linkage signal, consistent with a theoretical expectation.

Whether genetic associations and linkage peaks are caused by the same loci had been previously debated<sup>37</sup>. For example, a difference would be expected if family-specific mutations with large effects are the cause of the observed phenotype. Previous linkage studies in 20,240 sib-pairs failed to detect a colocalization between linkage signals and trait-associated SNPs from an independent GWAS of height and BMI in -130,000 individuals<sup>38</sup>. This lack of concordance could be the result of insufficient power in either or both linkage studies and GWASs. Our study revisited this observation using a new method, predLINK, and data from a fivefold larger linkage study and from currently the largest GWAS of height ( $N = 5$  million) and BMI ( $N = 650,000$ ). We show that observed and GWAS-predicted linkage signals are correlated across the genome, confirming that some of the same genetic loci contribute to within-family and population-wide genetic and phenotypic variance.

The heritability estimates for both height and BMI are remarkably similar to those estimated from twin studies<sup>1,28,29</sup>, despite the

experimental designs being orthogonal (between versus within families). This concordance suggests that assumptions underlying twin studies (for example, the 'equal environment' assumption for identical and nonidentical twin pairs) may not be strongly violated, at least for the traits studied. A large meta-analysis of twin studies across multiple complex traits concluded that the most parsimonious explanation of observed twin correlations was a simple model in which all familial correlations are the result of additive genetic variance<sup>1</sup>. Our results for height and BMI agree with that conclusion in that we find no evidence of a residual sibling covariance ( $c^2$ ) for BMI, whereas the significant  $c^2$  observed for height is largely explained by assortative mating. Nevertheless, we cannot rule out that the similarity of estimates from twin studies and within-family segregation for height and BMI is just a coincidence. Research involving more complex pedigrees and the analysis of multiple traits is needed to thoroughly test the congruence of estimates of both genetic segregation variance and genetic variance from the phenotypic correlation between relatives.

Our heritability estimates for height (0.76) and BMI (0.55) are significantly larger than 0.55 (s.e. = 0.04) and 0.29 (s.e. = 0.06) obtained by Young and colleagues<sup>15</sup> from data in Iceland, using their relatedness disequilibrium regression method (a generalization of the sibling IBD regression method to estimate heritability in a complex pedigree). It is interesting that their estimates from an analysis of a large collection of full sib-pairs ( $n = 56,461$ – $64,847$ ) were 0.68 (s.e. = 0.10) and 0.39 (s.e. = 0.12) for height and BMI, respectively, not significantly different from our estimates. There are many reasons why estimates of segregation variance from complex pedigrees could differ from those obtained using only nuclear families. First, although unaccounted interactions between genes and shared environment can yield biases in both contexts, the magnitude of these biases can differ across study designs if the amount of shared environment varies between first-degree and distant relatives. Moreover, estimates of additive genetic variance in a sibling design could also be biased upwards in the presence of dominance and epistatic effects, and any such bias is probably smaller in a complex pedigree. Yet there is little evidence of nonadditive genetic variance for height and BMI<sup>39,40</sup>. Moreover, our estimates of 0.76 and 0.55 can also be compared with estimates from GWAS and whole-genome sequencing (WGS) data. For height, the

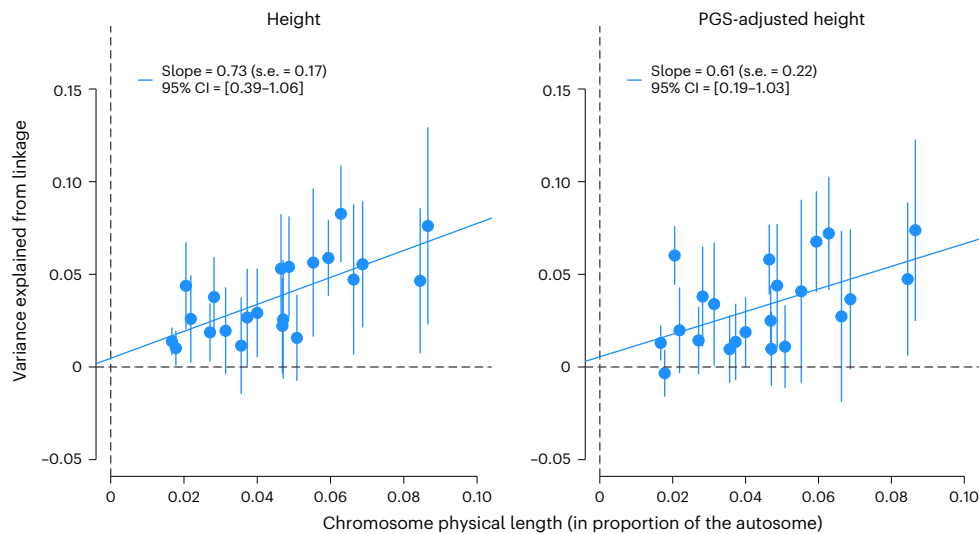


**Fig. 4 | Correlation between chromosome length and estimates of variance explained from linkage analyses of height.** Analyses were based on summary statistics from a linkage meta-analysis of height and height adjusted for PGSs in 119,457 QISPs. Each dot represents a chromosome. The x axis represents the physical length of each chromosome relative to the size of the autosome (that is, -2,879 Mb) and the y axis the expected variance explained ( $q_s^2$ ) for each chromosome ( $s = 1-22$ ) estimated as  $q_s^2 = m_s \bar{q}^2$ , where  $\bar{q}^2$  is the mean across the

chromosome of estimates of locus-specific variance and  $m_s$  an effective number of independent markers per chromosome (Supplementary Table 8). Error bars around each dot represent  $m_s \times$  the s.d. of the linkage estimate across the chromosomes. The s.e. values of the regression slopes were obtained using a leave-one-chromosome-out jackknife approach. The 95% CIs for the regression slopes were calculated as  $1.96 \times$  s.e.

SNP-based estimate is about 0.55–0.60 (ref. 41) and the WGS estimate -0.70 (ref. 42), but with a large s.e. = -0.10. These estimates imply that for height there is substantial genetic variation not captured by either SNP array and, to a lesser extent, sequence data, presumably ultra-rare variants (frequency <1 of 10,000 not included in ref. 42) and, perhaps, complex structural variation not captured by short-read sequencing technologies. For BMI, the gap is much larger, because estimates from both GWAS and WGS data are about 0.30 (refs. 41,42). Large exome studies have detected multiple genes with a significant burden of rare coding variants<sup>43,44</sup>, but these variants together explain a trivial amount of variation in the population. Our results after an adjustment for PGS imply that the remaining ('still-missing') genetic variation for height is also polygenic and not concentrated in a small number of genes. It is currently unknown what the genetic architecture of the remaining variants is in terms of allele frequency and effect sizes. All we can say for now is that they are not captured by common SNPs and large whole-exome sequencing studies. Future studies on WGS data and large sample sizes, for example, in the UKB, may be able to refine the genetic architecture for height and BMI and other complex traits.

The estimate of genetic trait variation from realized relationships is, per definition, within-family segregation variance. Usually, this variance is the same as genetic variance in the population. However, correlation across genes and environments, assortative mating and population stratification can all lead to a difference between population and within-family variance<sup>3</sup>. For height, and less so for BMI, there is strong evidence for assortative mating, including in the UKB<sup>45-47</sup>. In the presence of assortative mating, the estimate of heritability from 'sib regression', as used in our study, is biased downwards with respect to the heritability in the assortatively mating current population<sup>26</sup>. Therefore, if we account for assortative mating and assume that the resemblance between siblings is solely the result of genetic effects (and not of common environmental effects), then our data are consistent with a heritability of 0.87 (s.e. = 0.05) for height in the current population (Supplementary Note). Under these assumptions, the still-missing heritability for height is even larger.

Our genome-wide linkage scan detected several regions that traditionally would be termed 'significant' and followed up with

fine-mapping or candidate gene studies. This experimental design hypothesized that the cause of the linkage peak was a single genomic locus with one or more sequence variants of large effect which co-segregated with the trait in families. However, linkage analyses for complex traits were largely unsuccessful in identifying individual loci responsible for the observed linkage peaks. Our study provides strong empirical evidence that part, and perhaps most, of the explanation of the failure of the linkage design is that polygenic variation creates the appearance of 'major loci' when there are none. For example, the linkage peak for height on chromosome 10, which contains 69 independent height-associated SNPs (Table 1), disappears completely after adjustment for the PGS (Fig. 2). However, it is also possible that the clustering of height-associated SNPs at that locus is caused by an underlying structural variant partially tagged by each of those 69 SNPs<sup>33</sup>. If the null hypothesis being tested in linkage analysis is a highly polygenic model (for example, the infinitesimal model), instead of the traditional null hypothesis of no genetic variation anywhere in the genome, then the threshold for declaring a significant linkage peak would be larger and most declared 'significant' loci would probably disappear<sup>48</sup>.

There are several limitations to our study. First, even with more than 100,000 sibling pairs, the s.e. values of heritability estimates are still 0.05–0.07 and the linkage scans show large sampling variance (as shown in our simulations; Extended Data Fig. 2). The noncentrality parameter (NCP) of the  $\chi^2$  test to detect locus-specific linkage with a sib-pairs design is approximately  $nq^4(1+r_{\text{sib}}^2)/[8(1-r_{\text{sib}}^2)^2]$ , with  $n$  the number of sib-pairs,  $r_{\text{sib}}$  the phenotypic correlation between siblings and  $q^2$  the variance explained by a locus<sup>49,50</sup>. Therefore, if a gene contains multiple rare variants of large effect that cumulatively explain 0.5% of height variance (assuming  $r_{\text{sib}} \approx 0.5$ ), then at least 3.5 million sib-pairs would be required to yield 80% statistical power (at a 5% significance threshold) to detect linkage with that gene. Although the use of extended families (that is, beyond sib-pairs) could improve power, a large number of informative meioses are still needed. Second, we did not use a sex-specific recombination map in our RR-stratified analyses, which implies that our estimates might be affected by residual biases if height and BMI heritability are enriched at loci where RR varies between males and females. However, to the best of our knowledge, this is not supported by any evidence

and would warrant further investigations beyond the present study. Nevertheless, our RR-stratified framework can be easily extended to incorporate sex-specific information by using a partition of the genome that distinguishes loci with discordant RR between sexes. Third, our conclusions are limited to height and BMI because they are among the most commonly measured complex traits and, hence, provide the largest sample sizes. Fourth, our study focused on individuals of European ancestries because <5% of all sib-pairs available across cohorts could be assigned to other ancestry groups. Fifth, our investigation considered only autosomal genetic variation. Finally, future family-based studies on common disease and traits for which there is evidence of assortative mating and indirect genetic effects (for example, educational attainment) could provide estimates of genetic variance that are not confounded by such population-level effects. Supplementary Discussion addresses additional points about lack of power for analyses of the missing heritability of BMI (Table 2 and Extended Data Fig. 4) and the effect of dominance (Supplementary Table 12).

In conclusion, we report strong evidence of a high heritability of both height and BMI, consistent with inferences from twin and family studies. Our results imply a substantial still-missing heritability, that is, a large gap between the estimate of total additive genetic variation from our study and estimates of SNP heritability from GWAS data, in particular for BMI, where this gap is approximately 30% of phenotypic variance. We reconcile results from linkage and association studies, and show that ‘significant’ linkage peaks can be created from polygenic signals and that the still-missing heritability is also polygenic.

## Online content

Any methods, additional references, Nature Portfolio reporting summaries, source data, extended data, supplementary information, acknowledgements, peer review information; details of author contributions and competing interests; and statements of data and code availability are available at <https://doi.org/10.1038/s41588-024-01940-2>.

## References

- Polderman, T. J. C. et al. Meta-analysis of the heritability of human traits based on fifty years of twin studies. *Nat. Genet.* **47**, 702–709 (2015).
- Risch, N. & Merikangas, K. The future of genetic studies of complex human diseases. *Science* **273**, 1516–1517 (1996).
- Lynch, M. & Walsh, B. *Genetics and Analysis of Quantitative Traits* (Sinauer Associates, Inc., 1998).
- Botstein, D. & Risch, N. Discovering genotypes underlying human phenotypes: past successes for mendelian disease, future approaches for complex disease. *Nat. Genet.* **33**, 228–237 (2003).
- Hall, J. M. et al. Linkage of early-onset familial breast cancer to chromosome 17q21. *Science* **250**, 1684–1689 (1990).
- Goate, A. et al. Segregation of a missense mutation in the amyloid precursor protein gene with familial Alzheimer’s disease. *Nature* **349**, 704–706 (1991).
- Risch, N. J. Searching for genetic determinants in the new millennium. *Nature* **405**, 847–856 (2000).
- Weiss, K. M. & Terwilliger, J. D. How many diseases does it take to map a gene with SNPs? *Nat. Genet.* **26**, 151–157 (2000).
- Visscher, P. M., Brown, M. A., McCarthy, M. I. & Yang, J. Five years of GWAS discovery. *Am. J. Hum. Genet.* **90**, 7–24 (2012).
- McClellan, J. & King, M. C. Genetic heterogeneity in human disease. *Cell* **141**, 210–217 (2010).
- Klein, R. J., Xu, X., Mukherjee, S., Willis, J. & Hayes, J. Successes of genome-wide association studies. *Cell* **142**, 350–351 (2010).
- Wang, K., Bucan, M., Grant, S. F. A., Schellenberg, G. & Hakonarson, H. Strategies for genetic studies of complex diseases. *Cell* **142**, 351–353 (2010).
- Boyle, E. A., Li, Y. I. & Pritchard, J. K. An expanded view of complex traits: from polygenic to omnigenic. *Cell* **169**, 1177–1186 (2017).
- Visscher, P. et al. Assumption-free estimation of heritability from genome-wide identity-by-descent sharing between full siblings. *PLoS Genet.* **2**, e41 (2006).
- Young, A. I. et al. Relatedness disequilibrium regression estimates heritability without environmental bias. *Nat. Genet.* **50**, 1304–1310 (2018).
- Kong, A. et al. The nature of nurture: effects of parental genotypes. *Science* **359**, 424–428 (2018).
- Howe, L. J. et al. Within-sibship genome-wide association analyses decrease bias in estimates of direct genetic effects. *Nat. Genet.* **54**, 581–592 (2022).
- Lee, J. J. et al. Gene discovery and polygenic prediction from a genome-wide association study of educational attainment in 1.1 million individuals. *Nat. Genet.* **50**, 1112–1121 (2018).
- Smith, B. H. et al. Cohort profile: Generation Scotland: Scottish family health study (GS: SFHS). The study, its participants and their potential for genetic research on health and illness. *Int. J. Epidemiol.* **42**, 689–700 (2013).
- Scholtens, S. et al. Cohort profile: LifeLines, a three-generation cohort study and biobank. *Int. J. Epidemiol.* **44**, 1172–1180 (2015).
- Sijsma, A. et al. Cohort profile update: LifeLines, a three-generation cohort study and biobank. *Int. J. Epidemiol.* **51**, e295–e302 (2022).
- Bycroft, C. et al. The UK Biobank resource with deep phenotyping and genomic data. *Nature* **562**, 203–209 (2018).
- Leitsalu, L. et al. Cohort profile: Estonian Biobank of the Estonian Genome Center, University of Tartu. *Int. J. Epidemiol.* **44**, 1137–1147 (2015).
- Brumpton, B. M. et al. The HUNT study: a population-based cohort for genetic research. *Cell Genom.* **2**, 100193 (2022).
- Åsvold, B. O. et al. Cohort profile update: the HUNT study, Norway. *Int. J. Epidemiol.* **52**, e80–e91 (2023).
- Kemper, K. E. et al. Phenotypic covariance across the entire spectrum of relatedness for 86 billion pairs of individuals. *Nat. Commun.* **12**, 1050 (2021).
- Gazal, S. et al. Linkage disequilibrium-dependent architecture of human complex traits shows action of negative selection. *Nat. Genet.* **49**, 1421–1427 (2017).
- Schousboe, K. et al. Sex differences in heritability of BMI: a comparative study of results from twin studies in eight countries. *Twin Res.* **6**, 409–421 (2003).
- Silventoinen, K. et al. Heritability of adult body height: a comparative study of twin cohorts in eight countries. *Twin Res.* **6**, 399–408 (2003).
- Lander, E. & Kruglyak, L. Genetic dissection of complex traits: guidelines for interpreting and reporting linkage results. *Nat. Genet.* **11**, 241–247 (1995).
- Lander, E. S. & Botstein, D. Mapping mendelian factors underlying quantitative traits using RFLP linkage maps. *Genetics* **121**, 185–199 (1989).
- Dekkers, J. C. M. & Dentine, M. R. Quantitative genetic variance associated with chromosomal markers in segregating populations. *Theor. Appl. Genet.* **81**, 212–220 (1991).
- Yengo, L. et al. A saturated map of common genetic variants associated with human height. *Nature* **610**, 704–712 (2022).
- Yengo, L. et al. Meta-analysis of genome-wide association studies for height and body mass index in ~700000 individuals of European ancestry. *Hum. Mol. Genet.* **27**, 3641–3649 (2018).
- Visscher, P. M. Proportion of the variation in genetic composition in backcrossing programs explained by genetic markers. *J. Heredity* **87**, 136–138 (1996).
- Bulik-Sullivan, B. et al. An atlas of genetic correlations across human diseases and traits. *Nat. Genet.* **47**, 1236–1241 (2015).



37. Hodge, S. E. Linkage analysis versus association analysis: distinguishing between two models that explain disease-marker associations. *Am. J. Hum. Genet.* **53**, 367–384 (1993).
38. Hemani, G. et al. Inference of the genetic architecture underlying BMI and height with the use of 20,240 sibling pairs. *Am. J. Hum. Genet.* **93**, 865–875 (2013).
39. Hivert, V. et al. Estimation of non-additive genetic variance in human complex traits from a large sample of unrelated individuals. *Am. J. Hum. Genet.* **108**, 786–798 (2021).
40. Hill, W. G., Goddard, M. E. & Visscher, P. M. Data and theory point to mainly additive genetic variance for complex traits. *PLoS Genet.* **4**, e1000008 (2008).
41. Yang, J. et al. Genetic variance estimation with imputed variants finds negligible missing heritability for human height and body mass index. *Nat. Genet.* **47**, 1114–1120 (2015).
42. Wainschtein, P. et al. Assessing the contribution of rare variants to complex trait heritability from whole-genome sequence data. *Nat. Genet.* **54**, 263–273 (2022).
43. Backman, J. D. et al. Exome sequencing and analysis of 454,787 UK Biobank participants. *Nature* **599**, 628–634 (2021).
44. Akbari, P. et al. Sequencing of 640,000 exomes identifies GPR75 variants associated with protection from obesity. *Science* **373**, eabf8683 (2021).
45. Tenesa, A., Rawlik, K., Navarro, P. & Canela-Xandri, O. Genetic determination of height-mediated mate choice. *Genome Biol.* **16**, 269 (2016).
46. Yengo, L. et al. Imprint of assortative mating on the human genome. *Nat. Hum. Behav.* **2**, 948–954 (2018).
47. Robinson, M. R. et al. Genetic evidence of assortative mating in humans. *Nat. Hum. Behav.* **1**, 16 (2017).
48. Visscher, P. M. & Haley, C. S. Detection of putative quantitative trait loci in line crosses under infinitesimal genetic models. *Theor. Appl. Genet.* **93**, 691–702 (1996).
49. Sham, P. C., Cherny, S. S., Purcell, S. & Hewitt, J. K. Power of linkage versus association analysis of quantitative traits, by use of variance-components models, for sibship data. *Am. J. Hum. Genet.* **66**, 1616–1630 (2000).
50. Visscher, P. M. & Hopper, J. L. Power of regression and maximum likelihood methods to map QTL from sib-pair and DZ twin data. *Ann. Hum. Genet.* **65**, 583–601 (2001).

**Publisher's note** Springer Nature remains neutral with regard to jurisdictional claims in published maps and institutional affiliations.

Springer Nature or its licensor (e.g. a society or other partner) holds exclusive rights to this article under a publishing agreement with the author(s) or other rightsholder(s); author self-archiving of the accepted manuscript version of this article is solely governed by the terms of such publishing agreement and applicable law.

© The Author(s), under exclusive licence to Springer Nature America, Inc. 2024

<sup>1</sup>Institute for Molecular Bioscience, University of Queensland, Brisbane, Queensland, Australia. <sup>2</sup>QIMR Berghofer Medical Research Institute, Brisbane, Queensland, Australia. <sup>3</sup>Sorbonne University, Paris Brain Institute—ICM, CNRS, INRIA, INSERM, AP-HP, Hôpital de la Pitié Salpêtrière, Paris, France. <sup>4</sup>Institute of Clinical Medicine, Faculty of Medicine, University of Oslo, Oslo, Norway. <sup>5</sup>K.G. Jebsen Center for Genetic Epidemiology, Department of Public Health and Nursing, NTNU, Norwegian University of Science and Technology, Trondheim, Norway. <sup>6</sup>The Frazer Institute, University of Queensland, Woolloongabba, Queensland, Australia. <sup>7</sup>HUNT Research Centre, Department of Public Health and Nursing, NTNU, Norwegian University of Science and Technology, Levanger, Norway. <sup>8</sup>Department of Endocrinology, Clinic of Medicine, St Olavs Hospital, Trondheim, Norway. <sup>9</sup>Estonian Genome Centre, Institute of Genomics, University of Tartu, Tartu, Estonia. <sup>10</sup>Department of Epidemiology, University of Groningen, University Medical Center Groningen, Groningen, The Netherlands. <sup>11</sup>Department of Bioinformatics, Isfahan University of Medical Sciences, Isfahan, Iran. <sup>12</sup>MRC Human Genetics Unit, Institute of Genetics & Cancer, University of Edinburgh, Western General Hospital, Edinburgh, UK. <sup>13</sup>Centre for Genomic and Experimental Medicine, Institute of Genetics & Cancer, University of Edinburgh, Western General Hospital, Edinburgh, UK. <sup>14</sup>Human Genetics Department, David Geffen School of Medicine, University of California Los Angeles, Los Angeles, CA, USA. <sup>15</sup>Behavioral Decision Making Group, Anderson School of Management, University of California Los Angeles, Los Angeles, CA, USA. <sup>16</sup>National Bureau of Economic Research, Cambridge, MA, USA. <sup>17</sup>Department of Economics, New York University, New York, NY, USA. <sup>18</sup>Center for Experimental Social Science, New York University, New York, NY, USA. <sup>19</sup>MRC Integrative Epidemiology Unit, University of Bristol, Bristol, UK. <sup>20</sup>Centre for AgriBioscience, Agriculture Victoria, Bundoora, Victoria, Australia. <sup>21</sup>Faculty of Veterinary and Agricultural Sciences, University of Melbourne, Parkville, Victoria, Australia. <sup>22</sup>MRC Human Genetics Unit, Institute of Genetics and Cancer, University of Edinburgh, Western General Hospital, Edinburgh, UK. <sup>23</sup>Roslin Institute and Royal (Dick) School of Veterinary Studies, University of Edinburgh, Midlothian, UK. <sup>24</sup>Coupland Craft Cider, Coupland, Northumberland, UK. <sup>25</sup>Big Data Institute, Li Ka Shing Centre for Health Information and Discovery, Nuffield Department of Population Health, University of Oxford, Oxford, UK. <sup>26</sup>These authors jointly supervised this work: Peter M. Visscher, Loic Yengo.

✉ e-mail: [j.sidorenko@imb.uq.edu.au](mailto:j.sidorenko@imb.uq.edu.au); [peter.visscher@uq.edu.au](mailto:peter.visscher@uq.edu.au); [lyengo@imb.uq.edu.au](mailto:lyengo@imb.uq.edu.au)

## Estonian Biobank Research Team

Reedik Mägi<sup>9</sup> & Andres Metspalu<sup>9</sup>

Full lists of members and their affiliations appear in the Supplementary Information.

## Lifelines Cohort Study

Alireza Ani<sup>10,11</sup>, Rujia Wang<sup>10</sup>, Ilja M. Nolte<sup>10</sup> & Harold Snieder<sup>10</sup>

## Methods

### Ethics declaration

The research was carried out under the University of Queensland Institutional Human Research Ethics (UQ-HREC) approval no. UQ 2020/HE002938. Written informed consent was obtained from every participant in each study and the study was approved by relevant ethics committees. For the UKB study ethics approval was obtained from the North West Centre for Research Ethics Committee (no. 11/NW/0382). The HUNT study was approved by the Regional Committee for Medical and Health Research Ethics, Norway and all participants gave informed written consent (REK Central application no. 2018/2488). The LL was approved by the ethics committee of the University Medical Center Groningen, document no. METC UMCG METc 2007/152. The EBB is regulated by the Estonian Human Genes Research Act and all participants signed a broad informed consent form. The use of the information for the present study was approved by the Estonian Committee on Bioethics and Human Research (approval no. 1.1-12/1478). The QIMR studies were approved by the Human Research Ethics Committee of the QIMR Berghofer Medical Research Institute. Ethical approval for the GS Scottish Family Health Study (GS: SFHS) was obtained from the Tayside Committee on Medical Research Ethics A (ref. no. 05/S1401/89). GS obtained Research Tissue Bank approval from the East of Scotland Research Ethics Service (ref. no. 20/ES/0021).

### Genotyping and phenotyping

**Sample selection.** Genotypic and phenotypic information was collected for six large cohorts: the UKB<sup>22</sup> ( $N = 488,410$ ), GS<sup>19</sup> ( $N = 20,032$ ), the LL study<sup>20,21</sup> ( $N = 64,623$ ), the QIMR cohort ( $N = 13,154$ ), the EBB<sup>23</sup> ( $N = 197,582$ ) and the HUNT study<sup>24,25</sup> ( $N = 70,517$ ), where the sample size ( $N$ ) refers to the number of genotyped individuals before selection of siblings and quality control. Sample overlap ( $N = 622$ ) between GS and UKB was handled by removing the overlapping individuals from the UKB full-sib sample ( $N = 90$ ). We restricted our analyses to adult (that is, aged at least 18 years) full siblings of European ancestries with available phenotype measurements. Ancestry inference and sample exclusions are described in Supplementary Methods.

**Sibship inference.** We identified sib-pairs using the estimated kinship coefficients and, where available, pedigree information. In the UKB, the kinship coefficients and the proportion of markers for which pairs share no alleles (IBSO) were provided as a part of data release (estimated using KING<sup>51</sup> software) and were used to infer the sib-pairs following the procedure outlined in Bycroft et al.<sup>22</sup>. For all other cohorts, we similarly used the KING software (v.2.2.7; option '--related') to estimate pairwise kinship coefficients and to infer IBD-sharing segments for first-degree relationships, and then selected the inferred full-sib (FS) pairs using either SNP information (EBB, HUNT and LL) or both SNP and pedigree information where available (GS and QIMR). Consistent with previous studies<sup>14,38</sup>, we used a simplified data structure for our analyses by assuming sib-pairs to be independent even when the siblings involved were from the same family. We referred to those as quasi-independent sib-pairs (QISPs). For example, a sibship of four siblings would lead to  $4 \times 3/2 = 6$  QISPs included in our analysis. In total, 119,457 adult QISPs with available measures of height and/or BMI were taken forward for the analysis: 8,368 from GS, 12,844 from QIMR, 16,581 from LL, 21,756 from UKB, 25,333 from EBB and 34,575 from HUNT. Further details for each cohort are provided in Supplementary Table 13 and Supplementary Methods.

**SNP selection for IBD inference.** We selected approximately 25,000 directly genotyped and LD-independent SNPs per cohort to be used in the analysis, with an exception for LL data where high-quality (imputation  $r^2 > 0.9$ )-imputed, LD-independent HapMap3 markers were used (Supplementary Methods). SNP genotyping array, number of SNPs available for analysis, number of SNPs passing quality control steps and

$F_{ST}$  metrics are presented in Supplementary Table 14. Genomic positions used in the present study correspond to the hg19 genome build.

**Phenotype quality control.** Phenotype adjustments were performed within a sample of siblings in each cohort, separately for males and females. We set phenotype outliers ( $>6$  s.d. away from the mean) to missing and residualized phenotypes by fitting the age at assessment (AGE) as well as AGE<sub>2</sub> in a linear regression model as covariates. The phenotypes were then scaled to have a mean = 0 and a variance = 1 (or rank-based inverse normally transformed) within each sex. The cohort-specific phenotype means (before adjusting for fixed effects) and s.d. values (after adjusting for fixed effects, before scaling) are provided in Supplementary Table 15. The age distribution across cohorts is presented in Supplementary Table 16.

### IBD estimation and linkage analysis

**Estimation of IBD coefficients.** IBD coefficients between siblings were estimated along a grid of 0.5-cM spaced locations on each chromosome (genetic map positions from the interpolated CEU (northern Europeans from Utah) genetic map generated by the 1000 Genomes Project using OMNI arrays; 'Data availability') using the MERLIN<sup>52</sup> software package (v.1.1.2). Before IBD estimation, we detected and set unlikely genotypes to missing (--error function and pedwipe module in the MERLIN<sup>52</sup> software package, respectively). Using the estimated IBD probabilities, we further calculated the locus-specific, IBD-sharing proportions as  $\hat{\pi}_k = P_{1k}/2 + P_{2k}$ , where  $P_{1k}$  and  $P_{2k}$  are the probabilities of the siblings sharing one or two alleles identical by descent at locus  $k$ , respectively. For dominance IBD coefficients (IBD2), the proportion of sharing two alleles by descent was estimated as  $\hat{\pi}_{dk} = P_{2k}$ . Subsequently, the chromosome-wide IBD and IBD2 were estimated as an average of  $\hat{\pi}_k$  and  $\hat{\pi}_{dk}$ , respectively, across the chromosome grid locations. The genome-wide IBD was obtained as the length-weighted (length expressed in cM) average of chromosome-wide IBD coefficients. Coordinates on our genetic map (in cM) were converted to hg19 genomic positions to re-estimate IBD-sharing proportions in mega-base-pairs (Mb). The distributions of genome-wide and chromosome-wide IBD coefficients between siblings are presented for each cohort in Supplementary Table 2 and Supplementary Fig. 1.

**RR-stratified IBD coefficients.** We stratified the genome into four groups of 0.5-cM-long genomic segments corresponding to quartile groups of RRs within those segments. The RR within each segment was calculated as the ratio of its genetic length (that is, 0.5 cM) over its physical length in Mb, both obtained from the interpolated CEU genetic map used in our linkage analyses. The physical length and RR distribution across these segments are shown in Supplementary Fig. 2. IBD sharing within each RR-quartile group was calculated as the length-weighted (in cM or Mb) average of  $\hat{\pi}_k$  for segments allocated to that group.

**Genome-wide linkage analysis.** Locus-specific linkage analysis was performed along the same 0.5-cM grid using the Visscher–Hopper computationally fast regression approach<sup>50</sup>, which performs a weighted analysis of separate regressions of sibling, phenotypic, mean-centered squared differences and squared sums on their locus-specific estimated IBD coefficients. Significant linkage peaks were determined as when the LOD score at a given locus exceeds 3.6, as recommended previously<sup>30</sup>. The CIs for the location of causal variants underlying significant linkage peaks were calculated using the LOD drop-off method<sup>31</sup>. In brief, this method determines CIs by finding the genomic locations on both sides of the peak corresponding to a decrease in LOD score of 1 or 2 units. We conservatively chose a 2-unit LOD score drop-off to ensure a coverage of at least 95%.

**Heritability estimation.** We estimated  $h_{FS}^2$  and  $c^2$  (and dominance variance; Supplementary Table 12) in each cohort using the REstricted

Maximum Likelihood (REML) implemented in a customized R-script available on Zenodo ('Code availability').

### GWAS of BMI

We previously published a large GWAS of BMI<sup>34</sup> ( $N = 700,000$  participants) combining data from the GIANT consortium<sup>53</sup> (hereafter simply referred to as GIANT) and the UKB. To avoid biases resulting from the sample overlap with UKB (in particular for our prediction analyses), we regenerated GWAS summary statistics for BMI after excluding sib-pairs (and their relatives, defined as when the estimated genomic relationship exceeds 0.05) identified in the UKB. We then used the same analysis pipeline as Yengo et al.<sup>34</sup> after excluding that sample.

In brief, we first conducted a GWAS of BMI using BOLT-LMM v.2.4.1 (ref. 54), in a subsample of 397,279 UKB participants excluding sib-pairs and their relatives. The BMI phenotype was as described previously<sup>34</sup>. We analyzed SNPs from the third (v.3) release of imputed UKB data (imputed to the Haplotype Reference Consortium (HRC) and UK10K reference panel) with an imputation quality score  $>0.3$ . For each UKB participant, the genotypes were hard-called with posterior probability  $>0.9$  and removing SNPs with call rate  $>0.95$ ,  $P$  value for Hardy–Weinberg test  $>1 \times 10^{-5}$  and MAF = 0.001. We used a set of 561,573 HM3 SNPs (MAF 1% and LD pruned with  $r^2 > 0.9$ ) as 'model SNPs' to control for population structure and remaining relatedness in the sample. We then meta-analyzed our results from UKB with summary statistics from GIANT across a subset of ~1.1 million HM3 SNPs with MAF 1% and consistent alleles and allele frequencies (maximum absolute difference  $<0.15$ ) between the UKB and GIANT. Finally, we used Genome-wide Complex Trait Analysis (GCTA)<sup>55</sup> to perform a COnditional and JOint (COJO) analysis of summary statistics from the latter meta-analysis using a random sample of 50,000 UKB participants as LD reference. This analysis identified 795 conditionally and jointly significant SNPs at a genome-wide significant threshold  $P = 5 \times 10^{-8}$  (Supplementary Data), explaining ~5% of BMI variance. We then relaxed the significance threshold to  $P = 1 \times 10^{-3}$  to include 4,582 SNPs (Supplementary Data), collectively explaining ~9% of BMI variance (Table 2).

### Predicted linkage signal

For each chromosome, we predicted the expected linkage signal, measured as predicted variance explained,  $E[q_k^2]$ , at a given genetic position  $L_k$  (in morgans) using equation (1):

$$E[q_k^2] = \sum_{j=1}^M [2p_j(1-p_j)\beta_j^2] e^{-4|L_k-L_j|}, \quad (1)$$

where  $M$  is the number of causal SNPs on the chromosome and  $p_j$ ,  $\beta_j$  and  $L_j$  are the MAF, the minor allele effect and the genetic position of the  $j$ th causal SNP, respectively.

The intuition behind equation (1) is to predict linkage as the product between the variance explained by the  $j$ th causal SNP (that is,  $h_j^2 = 2p_j(1-p_j)\beta_j^2$ ) and the expected correlation  $r_{jk}$  between indicators that alleles at positions  $L_j$  and  $L_k$  are inherited by both siblings from the same parent<sup>14</sup>. Assuming Haldane's mapping function,  $r_{jk}$  can be expressed as  $r_{jk} = e^{-4|L_k-L_j|}$  (ref. 14). Then, the overall expectation  $E[q_k^2]$  is obtained by summing up the products  $h_j^2 r_{jk}$  across all causal SNPs on the chromosome. If each causal variant equally contributes to heritability, then equation (1) describes a discretized version of Dekkers and Dentine's<sup>32</sup> results obtained under an infinitesimal genetic architecture. We implemented this method in an R script available via Zenodo ('Code availability').

We used the same framework to derive an expectation of linkage signal even when causal variants were unknown by replacing causal SNPs with independent trait-associated SNPs identified from GWASs and causal SNP effects  $\beta_j$ , with the estimated joint SNP effects obtained from GWAS summary statistics using the GCTA-COJO module<sup>56</sup>. On average the number of trait-associated SNPs (for height and BMI) is

proportional to the length of the chromosome. Genetic distances were obtained using sex-averaged genetic map positions from the interpolated CEU genetic map generated by the 1000 Genomes Project from OMNI arrays ('Data availability'). We used 12,111 genome-wide significant SNPs jointly associated with height<sup>33</sup> and 795 genome-wide significant SNPs jointly associated with BMI (GWAS of BMI). Unique genetic positions on the CEU genetic map were available for 12,010 height-associated and 787 BMI-associated SNPs, and the allele frequencies were from the UKB sib-pair sample.

We assessed the accuracy of equation (1) to predict observed linkage signals by calculating Pearson's correlation between observed and expected linkage signals for each chromosome. We also reported the chromosome-length-weighted (length measured in cM) average of these correlations ( $\hat{\phi}$ ) across chromosomes. The s.e. of  $\hat{\phi}$  is calculated based on a leave-one-chromosome-out jackknife procedure using equation (2):

$$\text{s.e.}(\hat{\phi}) = \sqrt{\left(1 - \frac{1}{22}\right) \sum_{s=1}^{22} (\hat{\phi} - \hat{\phi}_{-s})^2}, \quad (2)$$

where  $\hat{\phi}_{-s}$  denotes the chromosome-length-weighted average across all chromosomes except chromosome  $s$ . Note that this s.e. does not capture sampling variation across individuals, but only tracks LD and genetic architecture differences between chromosomes.

### Simulated null distribution reflecting curvature effects

We first grouped all SNPs in the HapMap3 panel into 28 MAF–LD categories corresponding to 7 MAF classes (defined as:  $<1\%$ ; between 1% and 5%; between 5% and 10%; between 10% and 20%; between 20% and 30%; between 30% and 40%; and between 40% and 50%) and 4 LD classes (defined by quartile groups of the LD score distribution across HapMap3 SNPs). For each simulation replicate, we sampled the same number of SNPs as trait-associated SNPs present within each MAF–LD category. Finally, randomly sampled SNPs were allocated effect sizes that were also randomly sampled from the set of estimated SNP effects at trait-associated SNPs present in the corresponding MAF–LD category. We tested the statistical significance of the difference between  $\hat{\phi}$  and  $\hat{\phi}_{CE}$  using a Wald's test conditional on the observed value of  $\hat{\phi}$  (that is,  $\hat{\phi}$  is assumed to be fixed) and based on sampling variance of  $\hat{\phi}_{CE}$  across simulation replicates.

### PGSs and PGS-adjusted phenotypes

For each individual, we calculated the PGS based on the COJO effect estimates ( $\hat{\beta}_j$ , at SNP  $j$ ) of height- and BMI-associated SNPs from GWASs on ~650,000 ('GWAS of BMI') and  $>5$  million individuals<sup>33</sup>. We used 12,111 genome-wide significant SNPs for height and 4,582 SNPs with a less stringent  $P$ -value threshold ( $P = 1 \times 10^{-3}$ ) for BMI. We applied allelic scoring implemented in the PLINK v.1.90b6.20 software package<sup>57</sup> (--score option), to calculate the PGS of each individual included in our study. More specifically, the PGS of individual  $i$  (hereafter denoted  $\text{PGS}_i$ ) was calculated as  $\text{PGS}_i = \sum \hat{\beta}_j x_{ij}$ , where  $x_{ij}$  is the minor allele count of individual  $i$  at SNP  $j$  and  $\hat{\beta}_j$  the estimated effect of the minor allele at SNP  $j$ . In each cohort the imputed genotypes were used to extract available trait-associated SNPs. The imputation panel and the number of SNPs used in PGS calculations are reported in Supplementary Table 17 and the amount of variance explained by the PGS in each cohort is shown in Table 2.

### Estimation of SNP-based heritability

We estimated the SNP heritability of height and BMI in each cohort using the Genome-based Restricted Maximum Likelihood (GREML) method implemented in GCTA<sup>55</sup>. We calculated genomic relationship matrices (GRMs) using SNPs in the HapMap3 panel selected to have a MAF  $>0.01$  and  $P$  value for the Hardy–Weinberg equilibrium test  $>1 \times 10^{-6}$ . We hereafter refer to this GRM as the full GRM. We modeled shared genetic

and environmental effects between close relatives using another GRM obtained from the full GRM by setting all off-diagonal elements lower than 0.05 to 0. We used these two GRMs to jointly estimate the SNP-based heritability and the residual component capturing familial effects as done previously<sup>58</sup>. Sample sizes for these analyses are reported in Supplementary Table 13. SNP-based heritability estimates are shown in Table 2.

### Simulation of linkage studies

We performed simulations to assess the predictive performances of equation (1) under various genetic architectures. We simulated traits with a heritability  $h^2 = 1$  (to maximize statistical power) and varied the proportion of causal variants across the genome among 0.1%, 0.5%, 1%, 5%, 10%, 20%, 50% and 100%, thus defining eight different scenarios. All simulations were conditional on real data, as described below.

**Simulation of genotypes for IBD inference.** We simulated genotypes of 100,000 sib-pairs using phased haplotypes of 972 unrelated individuals in the UKB. As previously described<sup>49</sup>, phasing was performed with SHAPEIT v.2 (ref. 60) using genotypes of both parents for these 972 individuals, who were also participants of the UKB. We modified the R script proposed in ref. 59 (which initially focused on simulating inbreeding) to simulate sib-pairs. Our modified R script is available on Zenodo ('Code availability'). We simulated genotypes over 301,412 SNPs but focused our analyses on 26,136 LD-pruned (LD  $r^2 < 0.05$  in a 5-Mb window) SNPs with MAF  $> 10\%$ , consistent with our real data analysis in the UKB. Genetic positions were updated using the genetic maps downloaded from the Bcftools software website ('Data availability'). Genotypes were simulated once and then fixed across simulation replicates.

**Simulation of phenotypes.** Phenotypes were simulated conditionally on the simulated genotypes described above. Under each scenario (that is, proportion of causal variants) and for each simulation replicate, we randomly sampled  $M_c$  causal variants out of the 26,136 SNPs and then assigned each of them an allelic effect  $\beta_j$  (for causal SNP  $j$  with MAF  $p_j$ ) such that each causal SNP explains the same amount of trait variance. To achieve this, we set:

$$\beta_j = \sqrt{\frac{h^2}{2p_j(1-p_j)M_c}} \quad (3)$$

Next, we simulated the phenotype  $y_i$  of individual  $i$  using equation (4):

$$y_i = \sum_{j=1}^{M_c} \beta_j X_{ij}, \quad (4)$$

where  $X_{ij}$  is the minor allele count for individual  $i$  at causal SNP  $j$ . By construction the phenotypic variance is  $\text{var}(y_i) = h^2 = 1$ .

**Impact of estimation error in SNP effects from GWASs.** We assessed the impact on  $\hat{\phi}$  of errors in estimated causal SNP effects (Extended Data Fig. 2c) by replacing  $\beta_j$  with  $\hat{\beta}_j = \beta_j + \varepsilon_j$ , where  $\varepsilon_j$  is a random error term with mean = 0 and variance  $\sigma_{\hat{\beta}_j}^2$  defined as:

$$\sigma_{\hat{\beta}_j}^2 = \frac{1 - (h^2/M_c)}{2p_j(1-p_j)N_{R_g^2}} \quad (5)$$

In equation (5),  $N_{R_g^2}$  denotes the sample size of a hypothetical GWAS from which SNP effects were estimated. We chose  $N_{R_g^2} = R_g^2 / [M_c(1 - R_g^2)]$  such that the expected prediction accuracy of a PGS calculated from the  $\hat{\beta}_j$  values is  $R_g^2$  (ref. 61).

### Expected linkage test statistics under an infinitesimal genetic architecture

As in ref. 14, we determined for each chromosome an effective number ( $m_c$ ) of independent chromosomal segments (Supplementary Table 8). This number corresponds to the number of independent loci over

which the variance of IBD sharing would be equivalent to the observed variance for the whole genome. Note that the sum of  $m_c$  across chromosomes is  $m \approx 94$ , which is ~10% larger than that obtained by Visscher and colleagues<sup>14</sup> using microsatellites.

Under an infinitesimal genetic architecture, each of the  $m$  independent segments is expected to explain  $q^2 = \frac{h_{\text{IS}}^2}{m}$  of trait variance. Therefore, we used  $q^2$  to predict the NCP of the linkage test statistic ( $\chi^2$ ) across the genome as:

$$\text{NCP} = n \log \left\{ \frac{(1 - \rho_{1/2}^2)^{\frac{1}{2}}}{(1 - \rho_0^2)^{\frac{1}{4}} (1 - \rho_1^2)^{\frac{1}{4}}} \right\} \approx \frac{nq^4 (1 + r_{\text{sib}}^2)}{8(1 - r_{\text{sib}}^2)^2} \quad (6)$$

with  $n$  the number of sib-pairs and  $r_{\text{sib}}$  the phenotypic correlation between siblings,  $\rho_0 = r_{\text{sib}} - 0.5q^2$ ,  $\rho_{1/2} = r_{\text{sib}}$  and  $\rho_1 = r_{\text{sib}} + 0.5q^2$  (refs. 49,50), and thereby derived expectations for the mean and s.d. of  $\chi^2$  across loci as  $E[\chi^2] = 1 + \text{NCP}$  and  $\text{s.d.}(\chi^2) = \sqrt{2[1 + 2\text{NCP}]}$ . Finally, we predicted the proportion of test statistics with a positive value using the cumulative distribution function of the normal distribution with mean = 0 and variance equal to NCP.

### Reporting summary

Further information on research design is available in the Nature Portfolio Reporting Summary linked to this article.

### Data availability

Individual-level data used in the present study are available through application to the relevant cohort. The individual-level UKB data are available upon application to the UKB (<http://www.ukbiobank.ac.uk>, accessed under project no. 12505). Average IBD status across four groups of loci defined by quartiles of the RR distribution will be returned (to the UKB) for 21,756 sib-pairs analyzed in the present study. These data will be accessible to researchers registered with the UKB. A genetic map for linkage analyses of height and BMI was downloaded from [https://github.com/joepickrell/1000-genomes-genetic-maps/tree/master/interpolated\\_OMNI](https://github.com/joepickrell/1000-genomes-genetic-maps/tree/master/interpolated_OMNI). A genetic map used in simulations was obtained from Bcftools: <https://samtools.github.io/bcftools/bcftools.html>. Summary statistics from GWASs of BMI conducted in the present study are available in Supplementary Data and in the GWAS Catalog (<https://www.ebi.ac.uk/gwas>) under accession no. GCST90446645.

### Code availability

The customized code generated in this paper (source code of predLINK, R script to simulate sib-pairs, R script to run restricted maximum likelihood estimation for QISPs) is available via Zenodo at <https://doi.org/10.5281/zenodo.10416893> (ref. 62). All other analyses were performed using publicly available software. Statistical analyses were performed using R (v.4.1.0, v.4.2.1; <https://cran.r-project.org>). MERLIN v.1.1.2 software was used to estimate IBD sharing (<https://csg.sph.umich.edu/abecasis/Merlin/download/>). KING v.2.2.7 software was used to identify sib-pairs (<https://www.kingrelatedness.com/Download.shtml>). GWAS of BMI was performed using BOLT-LMM v.2.4.1 ([https://alkesgroup.broadinstitute.org/BOLT-LMM/BOLT-LMM\\_manual.html](https://alkesgroup.broadinstitute.org/BOLT-LMM/BOLT-LMM_manual.html)). GCTA software (gcta.1.93.1beta, v.1.93.2beta) was used for genotype data quality control (including principal component (PC) calculation, SNP loading calculation and PC projection for ancestry inference), SNP heritability estimation and COJO analysis (<https://yanglab.westlake.edu.cn/software/gcta/index.html>). Genotype data quality control, including filtering and LD pruning, as well as allelic scoring, was performed with PLINK v.1.90b6.20 (<https://www.cog-genomics.org/plink>).

### References

- Manichaikul, A. et al. Robust relationship inference in genome-wide association studies. *Bioinformatics* **26**, 2867–2873 (2010).

52. Abecasis, G. R., Cherny, S. S., Cookson, W. O. & Cardon, L. R. Merlin—rapid analysis of dense genetic maps using sparse gene flow trees. *Nat. Genet.* **30**, 97–101 (2002).
53. Locke, A. E. et al. Genetic studies of body mass index yield new insights for obesity biology. *Nature* **518**, 197–206 (2015).
54. Loh, P. R., Kichaev, G., Gazal, S., Schoech, A. P. & Price, A. L. Mixed-model association for biobank-scale datasets. *Nat. Genet.* **50**, 906–908 (2018).
55. Yang, J., Lee, S. H., Goddard, M. E. & Visscher, P. M. GCTA: a tool for genome-wide complex trait analysis. *Am. J. Hum. Genet.* **88**, 76–82 (2011).
56. Yang, J. et al. Conditional and joint multiple-SNP analysis of GWAS summary statistics identifies additional variants influencing complex traits. *Nat. Genet.* **44**, 369–375 (2012).
57. Chang, C. C. et al. Second-generation PLINK: rising to the challenge of larger and richer datasets. *Gigascience* **4**, 7 (2015).
58. Zaitlen, N. et al. Using extended genealogy to estimate components of heritability for 23 quantitative and dichotomous traits. *PLoS Genet.* **9**, e1003520 (2013).
59. Yengo, L., Wray, N. R. & Visscher, P. M. Extreme inbreeding in a European ancestry sample from the contemporary UK population. *Nat. Commun.* **10**, 3719 (2019).
60. Delaneau, O., Zagury, J.-F. & Marchini, J. Improved whole-chromosome phasing for disease and population genetic studies. *Nat. Methods* **10**, 5–6 (2013).
61. Wray, N. R. et al. Pitfalls of predicting complex traits from SNPs. *Nat. Rev. Genet.* **14**, 507–515 (2013).
62. Yengo, L. Genetic architecture reconciles linkage and association studies of complex traits. *Zenodo* <https://doi.org/10.5281/zenodo.10416893> (2023).

## Acknowledgements

We thank the participants and analysts in each cohort contributing to the present study. L.Y. was funded by the Australian Research Council (grant nos DE200100425 and FT220100069). P.M.V. was funded by the Australian Research Council (grant no. FL180100072) and the Australian National Health and Medical Research Council (NHMRC; grant no. 113400). B.C.-D. is supported by NHMRC's CJ Martin Fellowship (grant no. APP1161356). G.-H.M. is the recipient of an Australian Research Council Discovery Early Career Award (project no. DE220101226) funded by the Australian Government and supported by the Research Council of Norway

(project grant no. 325640). D.C. is supported by the Ragnar Söderberg Foundation (grant no. E42/15), D.C. and D.J.B. by Open Philanthropy (grant no. 010623-00001 to D.J.B.) and D.J.B. by the National Institute on Aging/National Institutes of Health (grant nos R24-AGO65184 and R01-AGO42568). D.M.E. is supported by an Australian NHMRC Investigator Award (no. 2017942). Additional acknowledgements are provided in Supplementary Information.

## Author contributions

P.M.V. and L.Y. conceptualized and jointly supervised the study. J.S. conducted statistical analyses (and meta-analyses) of UKB, QIMR, GS, LL and EBB data with assistance or guidance from P.M.V., L.Y. and K.E.K. G.-H.M. and B.B. performed linkage analyses using data from the HUNT study. B.C.-D., A.C., C.H., S.G., A.A., R.W., I.M.N., R.M., B.O.A. and L.B. prepared data in the respective cohorts. D.J.B., D.C., D.M.E., M.E.G. and C.S.H. contributed through suggestions and comments on study design, methods, analyses and their interpretation. D.P., S.E.M., N.G.M., H.S., A.M., K.H. and B.B. contributed to data collection, data management and scientific leadership of the respective cohorts. L.Y., P.M.V. and J.S. wrote the manuscript with the participation of all authors. All the authors approved the final version of the manuscript.

## Competing interests

The authors declare no competing interests.

## Additional information

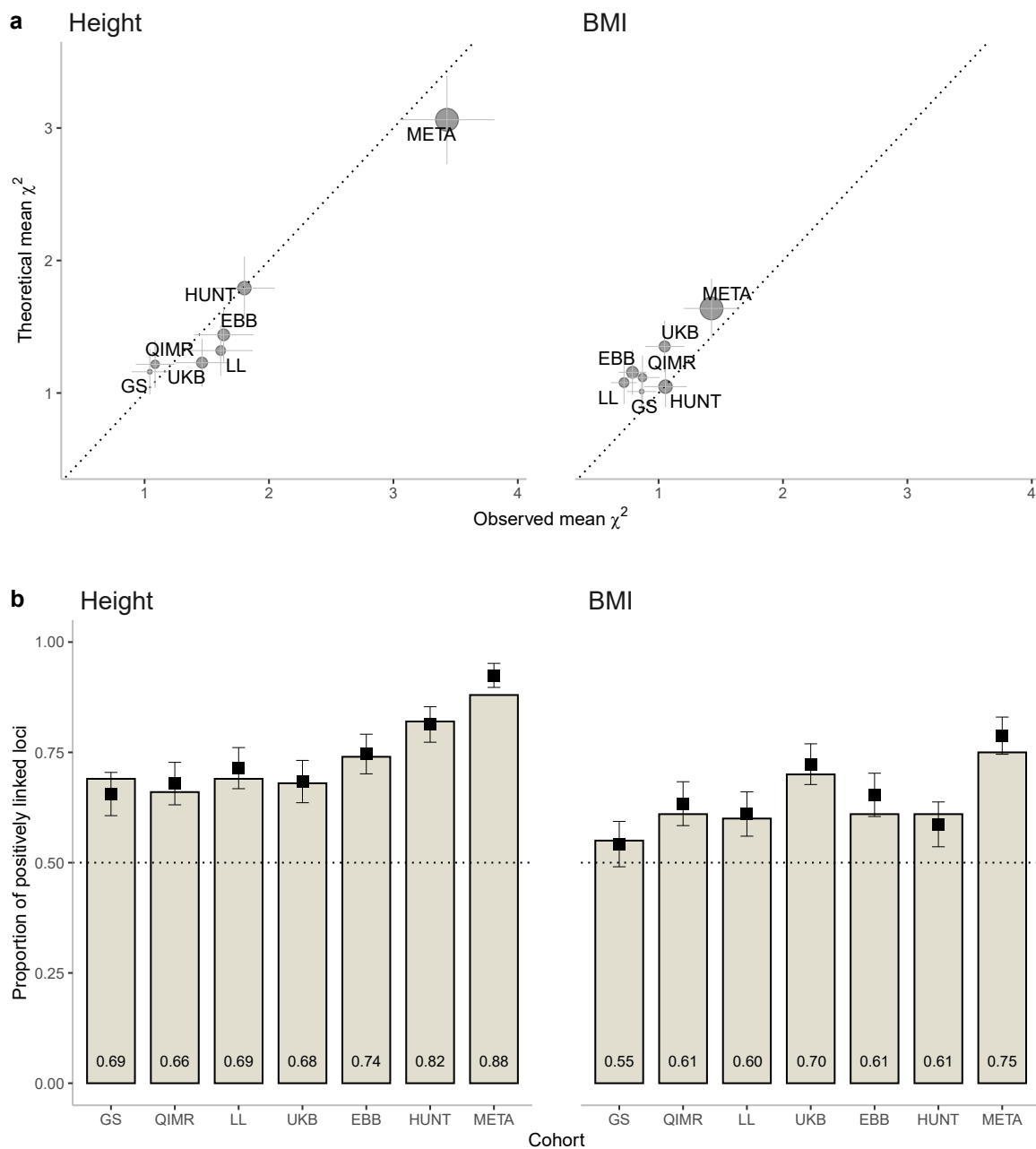
**Extended data** is available for this paper at <https://doi.org/10.1038/s41588-024-01940-2>.

**Supplementary information** The online version contains supplementary material available at <https://doi.org/10.1038/s41588-024-01940-2>.

**Correspondence and requests for materials** should be addressed to Julia Sidorenko, Peter M. Visscher or Loic Yengo.

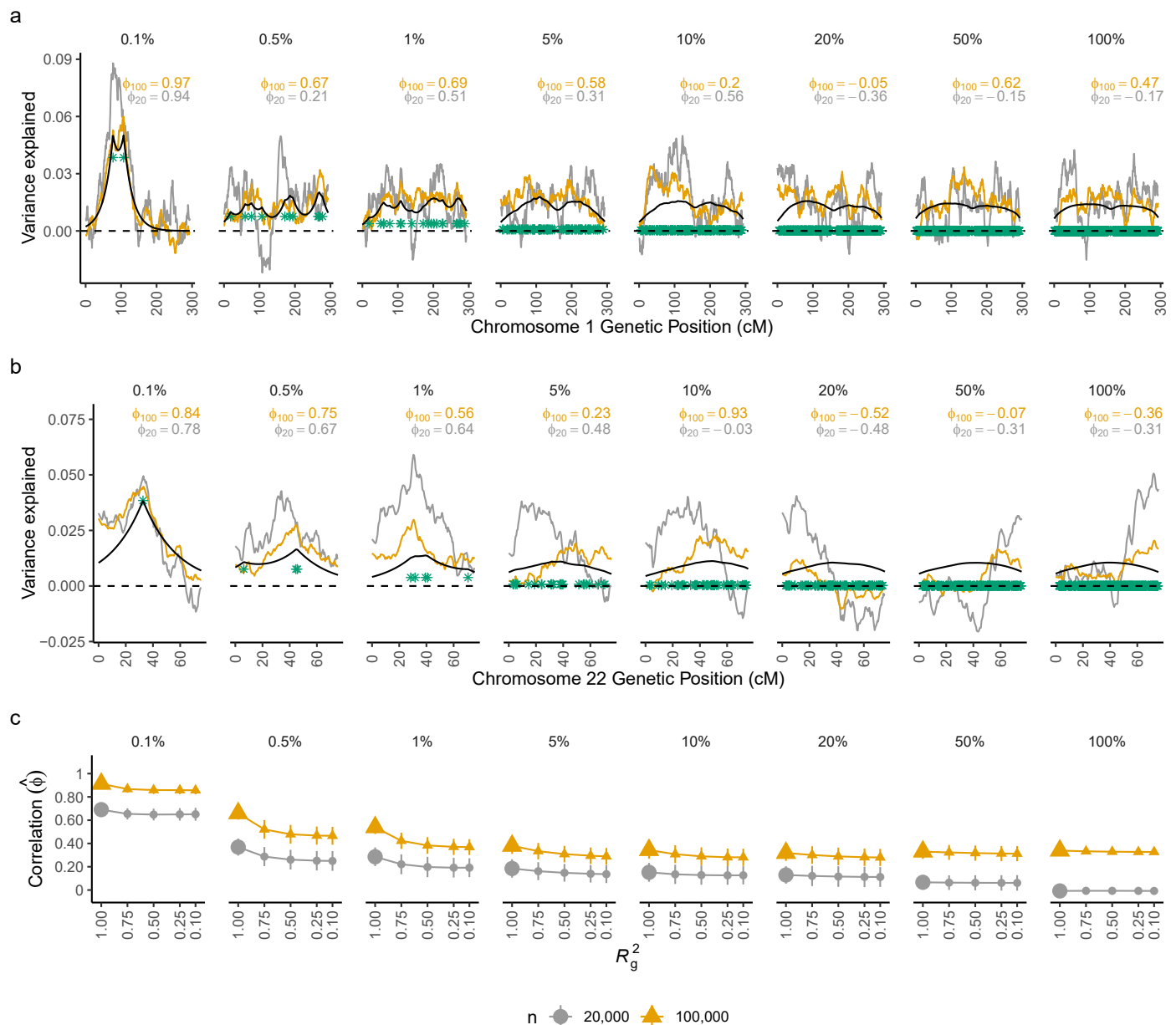
**Peer review information** *Nature Genetics* thanks Luke O'Connor, Daniel Weeks and the other, anonymous, reviewer(s) for their contribution to the peer review of this work. Peer reviewer reports are available.

**Reprints and permissions information** is available at [www.nature.com/reprints](http://www.nature.com/reprints).



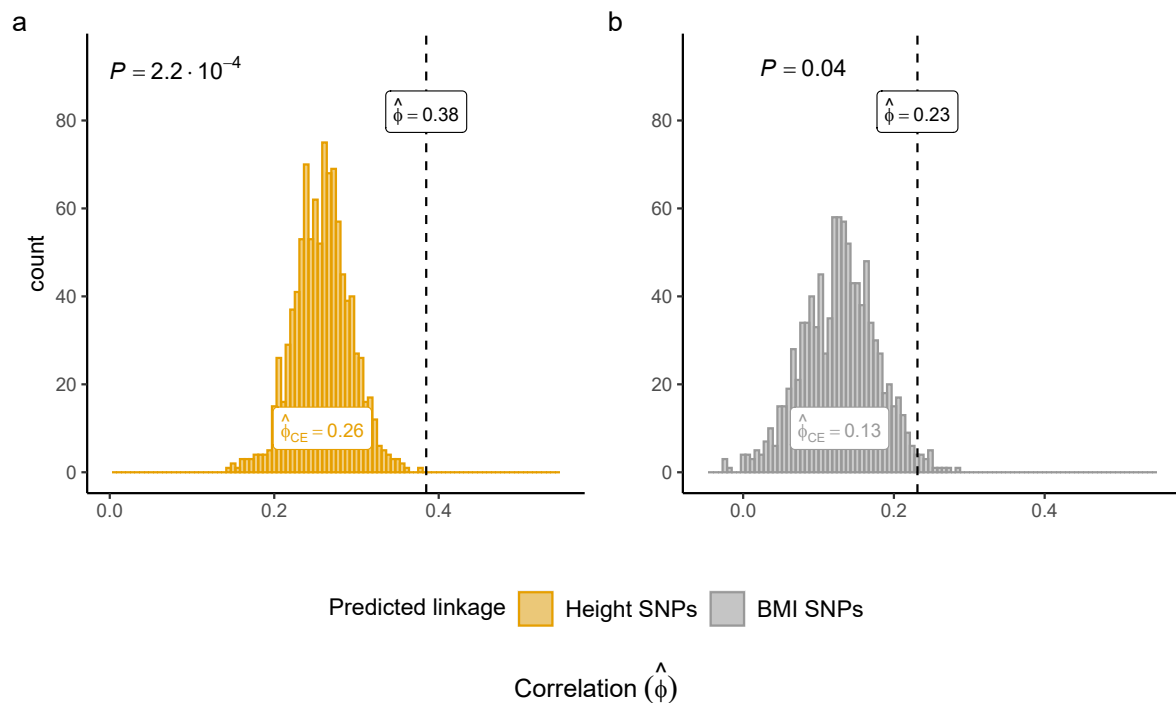
**Extended Data Fig. 1 | Observed and theoretically predicted statistics for locus-specific linkage analysis.** **a**, The observed and predicted mean test statistics of linkage ( $\chi^2$ ) test statistics for height and BMI. The error-bars indicate standard errors (s.e.) calculated as the standard deviation of locus-specific statistics divided by the square root of the effective number independent markers, that is  $\sim 94$  (Supplementary Table 8). The size of the circle is proportional to sample size. The theoretically predicted values are based on the REML estimates of heritability from genome wide IBD regression ( $\hat{h}_{IBD}^2$ ) and the observed correlation between siblings. **b**, The proportion of loci with positive (i) estimated linkage (the bars and the values) and (ii) theoretically predicted (the black

rectangles +/- s.e., Methods). The dotted horizontal line represents the proportion (that is, 0.5) expected in the absence of a genetic contribution to the trait. The data is shown for Generation Scotland (GS, number of quasi-independent sib-pairs ( $n$ ) = 8,368), the Queensland Institute of Medical Research cohort (QIMR,  $n$  = 12,844), the Lifelines Cohort (LL,  $n$  = 16,581), the UK Biobank (UKB,  $n$  = 21,756), the Estonian Biobank (EBB,  $n$  = 25,333) the HUNT study (HUNT,  $n$  = 34,575) and the meta-analysis combining all cohorts (META,  $n$  = 119,457). The numerical values for mean and median  $\chi^2$  and proportion of  $\chi^2 > 0$  are presented in Supplementary Table 7a.



**Extended Data Fig. 2 | Effect of polygenicity and sample size of linkage studies on the correlation between predicted and observed linkage signals in simulated data.** The results are shown for 8 simulated genetic architectures (polygenicity = 0.1%–100%) with a genome-wide  $h^2 = 1$ . **a–b**, show the observed and predicted linkage signals (measured as variance explained) on chromosomes 1 (**a**) and 22 (**b**), respectively, for one simulation replicate. The simulated causal variants are depicted as green stars. The predicted signal, estimated as a weighted sum of simulated effects (Methods, equation (1)) is depicted by the black curve. The grey and yellow lines show the observed linkage signal from the analysis of 20,000 and 100,000 simulated sib-pairs, respectively, where the phenotypes were simulated using the same causal variants (green stars). The correlations  $\hat{\phi}$  for each polygenicity panel are the chromosome-wide estimates for each linkage sample size (yellow:  $n=20,000$ ; grey:  $n=100,000$ ). **c**, the

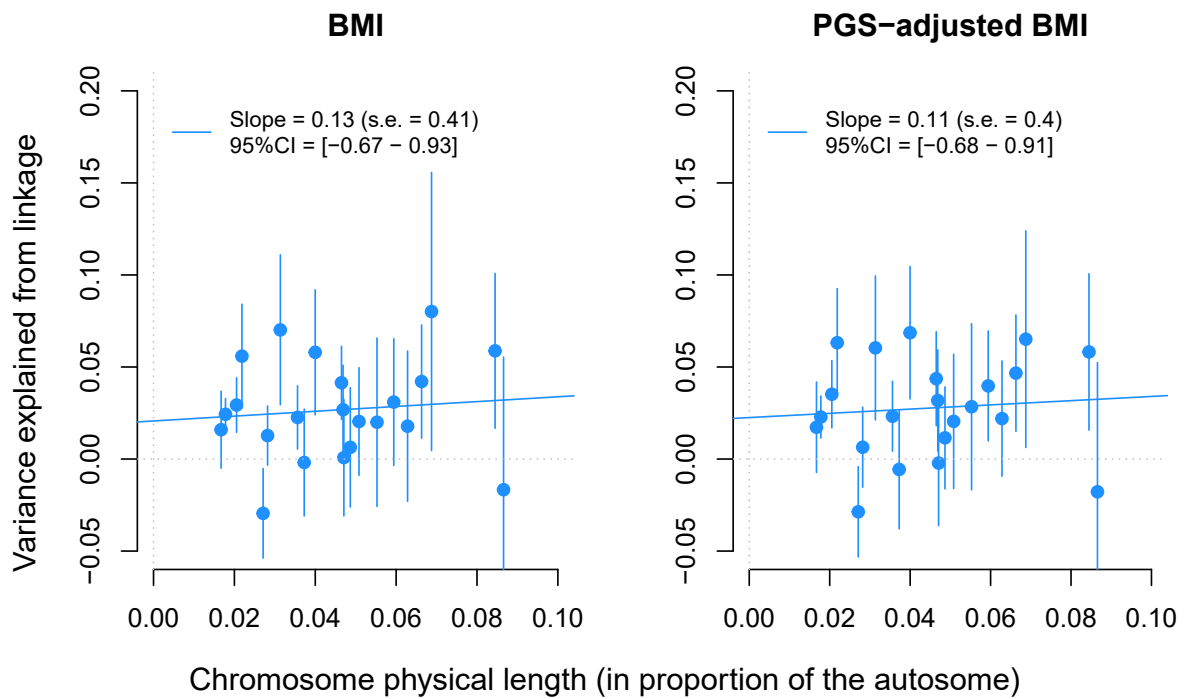
summary of results across 100 replicates.  $\hat{\phi}$  is estimated per chromosome across the grid of 0.5 cM, then a chromosome length weighted average is calculated for each replicate. Each symbol represents a mean value across 100 simulation replicates and the error bars are standard deviation across replicates. The left-most enlarged symbols for each polygenicity panel indicate that the true simulated SNP effects were used to predict linkage signal, that is, the expected prediction accuracy from polygenic scores ( $R_g^2$ ) using these causal variants = 1. To approximate estimation errors of SNP effects in a GWAS of finite sample,  $\hat{\phi}$  was also calculated using causal variants with  $R_g^2 < 1$  (regular symbols). For the numeric values see Supplementary Table 9. Estimated variance components were not constrained to ensure unbiasedness. Therefore, if a region of the genome does not explain any genetic variation, then 50% of the estimates are expected to be negative.



**Extended Data Fig. 3 | Colocalization between GWAS-predicted and observed linkage signals for traits adjusted for polygenic scores (PGS).** **a**, The correlation between observed linkage signals for PGS-adjusted height and predicted linkage signals from 12,010 height-associated SNPs. **b**, The correlation between observed linkage signals for PGS-adjusted BMI and predicted linkage signals from 787 BMI-associated SNPs. Height was adjusted using a PGS based on the same 12,010 height-associated SNPs (explaining 38% of height variance), while BMI was adjusted using a PGS including 4,582 SNPs (explaining 9% of BMI variance). The x-axis in each panel displays the correlation ( $\hat{\phi}$ ) between observed and predicted (from GWAS results; Methods) linkage signals. In each panel, the vertical dashed line represents the correlation between observed and predicted linkage signals from either height-associated SNPs (**a**) or 787 BMI-associated

SNPs (**b**). Predicted linkage signals were also obtained under the null hypothesis (that is ‘the correlation between observed and predicted linkage signals is due to the curvature effect’) using 1,000 draws of random SNPs with similar minor allele frequency and linkage disequilibrium properties as trait-associated SNPs. The histogram in each panel represents the distribution of correlations (under the null) between observed linkage for the trait indicated in the corresponding column-panel and predicted linkage obtained from these 1,000 draws. The mean of correlations obtained under the null hypothesis is denoted  $\hat{\phi}_{CE}$ . The  $P$ -values ( $P$ ) reported in the top-left corner of each panel assess the statistical significance of the difference between  $\hat{\phi}$  and  $\hat{\phi}_{CE}$  using a two-sided Wald test. Numeric values are presented in Supplementary Table 10.





**Extended Data Fig. 4 | Correlation between chromosome length and estimates of variance explained from linkage analyses of BMI.** Analyses were based on summary statistics from a linkage meta-analysis of BMI and BMI adjusted for polygenic score (PGS). The  $x$  axis represents the physical length of each chromosome relative to the size of the autosome (that is, -2879 Mb). The  $y$  axis represents the expected variance explained ( $q_s^2$ ) for each chromosome ( $s = 1-22$ ) estimated as  $q_s^2 = m_s \bar{q}^2$ , where  $\bar{q}^2$  is the mean across the chromosome

of estimates of locus-specific variance, and  $m_s$  an effective number of independent markers per chromosome (Supplementary Table 8). Error bars around each dot represent  $m_s$  times the standard deviation of linkage estimate across the chromosomes. Standard errors (s.e.) of the regression slopes were obtained using a leave-one-chromosome-out jackknife approach. 95% confidence intervals (CI) were calculated as  $1.96 \times \text{s.e.}$

## Reporting Summary

Nature Portfolio wishes to improve the reproducibility of the work that we publish. This form provides structure for consistency and transparency in reporting. For further information on Nature Portfolio policies, see our [Editorial Policies](#) and the [Editorial Policy Checklist](#).

### Statistics

For all statistical analyses, confirm that the following items are present in the figure legend, table legend, main text, or Methods section.

- |                                     |  |
|-------------------------------------|--|
| n/a                                 | Confirmed  |
| <input type="checkbox"/>            | <input checked="" type="checkbox"/> The exact sample size ( $n$ ) for each experimental group/condition, given as a discrete number and unit of measurement  |
| <input checked="" type="checkbox"/> | <input type="checkbox"/> A statement on whether measurements were taken from distinct samples or whether the same sample was measured repeatedly   |
| <input type="checkbox"/>            | <input checked="" type="checkbox"/> The statistical test(s) used AND whether they are one- or two-sided<br><i>Only common tests should be described solely by name; describe more complex techniques in the Methods section.</i>   |
| <input type="checkbox"/>            | <input checked="" type="checkbox"/> A description of all covariates tested   |
| <input type="checkbox"/>            | <input checked="" type="checkbox"/> A description of any assumptions or corrections, such as tests of normality and adjustment for multiple comparisons  |
| <input type="checkbox"/>            | <input checked="" type="checkbox"/> A full description of the statistical parameters including central tendency (e.g. means) or other basic estimates (e.g. regression coefficient) AND variation (e.g. standard deviation) or associated estimates of uncertainty (e.g. confidence intervals) |
| <input type="checkbox"/>            | <input checked="" type="checkbox"/> For null hypothesis testing, the test statistic (e.g. $F$ , $t$ , $r$ ) with confidence intervals, effect sizes, degrees of freedom and $P$ value noted<br><i>Give <math>P</math> values as exact values whenever suitable.</i>                            |
| <input checked="" type="checkbox"/> | <input type="checkbox"/> For Bayesian analysis, information on the choice of priors and Markov chain Monte Carlo settings  |
| <input checked="" type="checkbox"/> | <input type="checkbox"/> For hierarchical and complex designs, identification of the appropriate level for tests and full reporting of outcomes  |
| <input type="checkbox"/>            | <input checked="" type="checkbox"/> Estimates of effect sizes (e.g. Cohen's $d$ , Pearson's $r$ ), indicating how they were calculated   |

*Our web collection on [statistics for biologists](#) contains articles on many of the points above.*

### Software and code

Policy information about [availability of computer code](#)

Data collection

Data analysis https://zenodo.org/records/10416893) implementing a fast version and memory efficient version of restricted maximum likelihood estimation for heritability in quasi-independent siblings pairs."/>

For manuscripts utilizing custom algorithms or software that are central to the research but not yet described in published literature, software must be made available to editors and reviewers. We strongly encourage code deposition in a community repository (e.g. GitHub). See the Nature Portfolio [guidelines for submitting code & software](#) for further information.

## Data

Policy information about [availability of data](#)

All manuscripts must include a [data availability statement](#). This statement should provide the following information, where applicable:

- Accession codes, unique identifiers, or web links for publicly available datasets
- A description of any restrictions on data availability
- For clinical datasets or third party data, please ensure that the statement adheres to our [policy](#)

We used genotypic data and phenotypic data from the UK biobank (under project number 12505), Generation Scotland Cohort, the Lifelines Cohort Study, the QIMR Cohort Study, the Estonian Biobank and the HUNT Study. Individual-level data from the UK Biobank can be accessed upon request once a research project has been submitted and approved by the UKB research committee. Individual-level data from other cohorts (except HUNT) can be accessed upon approval of a specific research proposal. Genome-wide association summary statistics generated from this study will be made available for download from <https://cnsgenomics.com/data/>.

## Research involving human participants, their data, or biological material

Policy information about studies with [human participants or human data](#). See also policy information about [sex, gender \(identity/presentation\), and sexual orientation](#) and [race, ethnicity and racism](#).

Reporting on sex and gender	We analyzed data from all participants regardless of their sex or gender. Analyses of autosomal variants were adjusted for sex by using it as a covariate in regression models.
Reporting on race, ethnicity, or other socially relevant groupings	Study participants were assigned European ancestry using principal components analyses of their genotypes. Principal components were used to determine genetic proximity to a reference sample of 504 individuals in the 1000 Genomes Project, whose ancestry group was broadly defined as European.
Population characteristics	Analyses in each cohort was adjusted for age, age square and sex. The distribution (mean and standard deviation) of height and body mass index is provided in Supplementary 15 for separately for male and female participants of each cohort. Supplementary 15 also reports the sex distribution in each cohort. The age distribution across cohorts is summarized in Supplementary Table 16.
Recruitment	<p>UK Biobank: UK Biobank investigators sent postal invitations to 9,238,453 individuals registered with the UK's National Health Service who were aged 40–69 years and lived within approximately 25 miles (40 km) of one of 22 assessment centers located throughout England, Wales, and Scotland. Overall, 503,317 participants consented to join the study cohort and visited an assessment center between 2006 and 2010, resulting in a participation rate of 5.45%. (Fry et al. Am J Epidemiol. 2017 Nov 1;186(9):1026-1034).</p> <p>HUNT is an ongoing population-based health study in Trøndelag County, Norway. The study collects health-related data from questionnaires, interviews, and clinical examinations from individuals within that geographical region. More than 229,000 adults (20 years or older at recruitment) have participated in the study to date, of whom 95,000 have provided at least one biological sample. The periodic survey design includes four recruitment waves. More details about the study recruitment is given in Brumpton et al. (2022) Cell Genomics (2)10:100193.</p> <p>Lifelines is a multigenerational cohort study including over 167,000 participants (i.e., 10% of the northern population of the Netherlands) aged at least 13 years. Details about the cohort and data collection protocols are available at <a href="https://www.lifelines.nl/researcher/data-and-biobank">https://www.lifelines.nl/researcher/data-and-biobank</a>.</p> <p>The Estonian Biobank cohort is a volunteer-based sample of the Estonian resident adult population (aged ≥18 years). The current number of participants around 200,000. Details about the study design are available in Leitsalu et al. (2015), IJE 44 (4): 1137 - 1147.</p> <p>Queensland Twin Registry (QTwin) Study is a volunteer-based population-based registry of identical and non-identical twins and triplets of all ages, living in Australia. Details about the study at <a href="https://www.qimrberghofer.edu.au/qtwin/">https://www.qimrberghofer.edu.au/qtwin/</a></p> <p>The Generation Scotland: Scottish Family Health Study (GS:SFHS) is a family-based population cohort with DNA, biological samples, socio-demographic, psychological and clinical data from approximately 24,000 adult volunteers across Scotland. Details about that study are available in Nagy et al. (2017) - Genome Med 9(1):23.</p>
Ethics oversight	The research was carried out under the University of Queensland Institutional Human Research Ethics (UQ-HREC) Approval Number UQ 2020/HE002938. Written informed consent was obtained from every participant in each study, and the study was approved by relevant ethics committees. UKB: Ethics approval for the UK Biobank study was obtained from the North West Centre for Research Ethics Committee (11/NW/0382). HUNT: The HUNT Study was approved by the Regional Committee for Medical and Health Research Ethics, Norway and all participants gave informed written consent (REK Central application number 2018/2488). Lifelines Study: The Lifelines study was approved by the ethics committee of the University Medical Center Groningen, document number METC UMCG METc 2007/152. EBB: Estonian Biobank is regulated by the Estonian Human Genes Research Act (HGRA) and all participants have signed broad informed consent form. The use of the information for this study was approved by the Estonian Committee on Bioethics and Human Research (approval No 1.1-12/1478). QIMR: The QIMR studies were approved by the Human Research Ethics Committee of the QIMR Berghofer Medical Research Institute. GS: Ethical approval for the GS:SFHS study was obtained from the Tayside Committee on Medical

Note that full information on the approval of the study protocol must also be provided in the manuscript.

## Field-specific reporting

Please select the one below that is the best fit for your research. If you are not sure, read the appropriate sections before making your selection.

Life sciences  Behavioural & social sciences  Ecological, evolutionary & environmental sciences

For a reference copy of the document with all sections, see [nature.com/documents/nr-reporting-summary-flat.pdf](https://www.nature.com/documents/nr-reporting-summary-flat.pdf)

## Life sciences study design

All studies must disclose on these points even when the disclosure is negative.

Sample size	We analyzed data from all European ancestries quasi-independent sibling pairs (QISP) available in UK Biobank (N=21,756 QISP), Generation Scotland (N=8,368 QISP), Lifelines COhort Study (N=16,581 QISP), QIMR (N=12,844 QISP), Estonian Biobank (N=25,333 QISP) and HUNT Study (N=34,575 QISP).
Data exclusions	We focused on European ancestry participants (to ensure the largest sample size) aged over 18 with available measures of height and body mass index and genotyping missingness rate lower than 5%. Phenotypic values larger than 6 standard deviation away from the mean (in the sample) were discarded.
Replication	We did not attempt to replicate our findings in another sample given the large power required to replicate linkage studies. We discuss differences in heritability estimates from Young et al. (2018) 50(9):1304-1310.
Randomization	N/A - Rationale: No intervention was implemented on study participants. We used all available data whenever available.
Blinding	N/A - Rationale: No intervention was implemented on study participants.

## Reporting for specific materials, systems and methods

We require information from authors about some types of materials, experimental systems and methods used in many studies. Here, indicate whether each material, system or method listed is relevant to your study. If you are not sure if a list item applies to your research, read the appropriate section before selecting a response.

### Materials & experimental systems

### Methods

- n/a Involved in the study
- Antibodies
  - Eukaryotic cell lines
  - Palaeontology and archaeology
  - Animals and other organisms
  - Clinical data
  - Dual use research of concern
  - Plants

- n/a Involved in the study
- ChIP-seq
  - Flow cytometry
  - MRI-based neuroimaging

## Plants

Seed stocks	N/A
Novel plant genotypes	N/A
Authentication	N/A